DOE/ER/60674-8

DOE/ER/60674--8

BASE SEQUENCE EFFECTS ON DNA REPLICATION INFLUENCED BY BULKY ADDUCTS

FINAL REPORT

For the period March 1, 1995 to February 28, 1997

N.E. Geacintov

Chemistry Department
New York University
New York, NY 10003

Tel (212) 998 8407
Fax (212) 998 8421
E-Mail: geacinto@is.nyu.edu

NOTICE

May 31, 1997

Prepared for the Department of Energy
Agreement No. DE-FGO2-88ER60674

ABSTRACT

Polycyclic aromatic hydrocarbons (PAH) are environmental pollutants that are present in our air, food, and water. While PAH compounds are chemically inert and are sparingly soluble in aqueous solutions, in living cells they are metabolized to a variety of oxygenated derivatives, including the highly mutagenic and tumorigenic diol epoxide derivatives. The diol epoxides of the sterically hindered fjord region compound benzo[c]phenanthrene (B[c]PhDE) are among the most powerful tumorigenic compounds in animal model test systems. In this project, site-specifically modified oligonucleotides containing single B[c]PhDE-N^6-dA lesions derived from the reactions of the 1S,2R,3R,4S and 1R,2S,3S,4R diol epoxides of B[c]PhDE with dA residues were synthesized. The replication of DNA catalyzed by a prokaryotic DNA polymerase (the exonuclease-free Klenow fragment *E. Coli* Pol I) in the vicinity of the lesion at base-specific sites on B[c]PhDE-modified template strands was investigated in detail. The Michaelis-Menten parameters for the insertion of single deoxynucleotide triphosphates into growing DNA (primer) strands using the modified dA* and the bases just before and after the dA* residue as templates, depend markedly on the stereochemistry of the B[c]PhDE-modified dA residues. These observations provide novel insights into the mechanisms by which bulky PAH-DNA adducts affect normal DNA replication.

BASE-SPECIFIC AND STEREOCHEMICAL EFFECTS OF BULKY B[c]PhDE LESIONS ON POLYMERASE-CATALYZED DNA SYNTHESIS *In Vitro*

1. Background

Benzo[c]phenanthrene, like other PAH compounds (Conney, 1982), can be metabolically activated to highly reactive, mutagenic and tumorigenic diol epoxide derivatives (Ittah et al., 1983; Thakker et al., 1986; Pruess-Schwartz et al., 1987) that bind to cellular DNA (Dipple et al., 1987; Agarwal et al., 1987, 1996; Einolf et al., 1996). The most important ultimate mutagenic and tumorigenic metabolites of B[c]Ph are the "fjord-region" diol epoxide isomers, 3,4-dihydroxy-1,2-epoxy 1,2,3,4-tetrahydro benzo[c]phenanthrene (B[c]PhDE). There are two diaestereomeric forms, *syn*-B[c]PhDE and *anti*-B[c]PhDE. Each diastereomer can be resolved into a pair of chiral stereoisomers; for example, *anti*-B[c]PhDE can be resolved into two stereoisomers; the (+)-4S,3R,2R,1S- and the (-)-4R,3S,2S,1R-*anti*-enantiomers. B[c]PhDE binds more strongly to deoxyadenosine (dA) residues in native DNA *in vitro* (Agarwal et al., 1987, 1996; Dipple et al., 1987) and in rodent embryo cell cultures (Pruess-Schwartz et al., 1987) and forms covalent B[c]PhDE-N^6-dA adducts (Einolf et al., 1996).

The B[c]PhDE stereoisomers are characterized by differences in their mutagenic and tumorigenic activities (Wood et al., 1984; Bigger et al., 1989; 1992; Levin et al., 1986). The enantiomeric B[c]PhDE isomers exhibit different biological activities: for example, tumorigenic assays in newborn mice have shown that (-)-*anti*-B[c]PhDE was almost 10-fold more active in producing lung tumors than (+)-*anti*-B[c]PhDE, whereas the mutagenesis assays in the *supF* gene shows that the (+)-*anti*-enantiomer is more mutagenic than the (-)-*anti*-enantiomer. The relationships between the structures of the B[c]PhDE-DNA adducts and the biological consequences associated with these lesions are of great interest for understanding the relationships between molecular structure and mutagenic activity. Because of the variety of adducts that are formed when B[c]PhDE reacts with DNA (Dipple et al., 1987; Agarwal et al., 1987) and the effects of base sequence on reactivity and biological activity (Ross et al., 1993), it is important to use site-specific and stereochemically well-defined lesions embedded in defined DNA sequences for studies of structure-biological activity relationships.

In this work, we have selected site-specific and stereospecific B[c]PhDE-N^6-dA adducts as our model system in the study of biological activities *in vitro* because of the following two reasons: (1) We have successfully used the direct synthesis method to synthesize stereochemically defined (+) and (-)-*trans-anti*-B[c]PhDE-N^6-dA lesions site-specifically placed in oligonucleotides (Laryea 1995, Cosman et al., 1993, 1995). (2) The solution NMR characteristics of these lesions in the double-stranded oligonucleotides d(CTCC[$A^{B[c]PhDE}$]CTTCC). d(GGAAGTGAGAG) have already been reported (Cosman et al., 1993, 1995). The distinct conformational features of B[c]PhDE-N^6-dA lesions in DNA duplexes are the following: in *the* (+)-*trans-anti*-B[c]PhDE-N^6-dA adduct, the polycyclic aromatic B[c]Ph residue intercalates between adjacent base pairs on the 5'-side of the modified

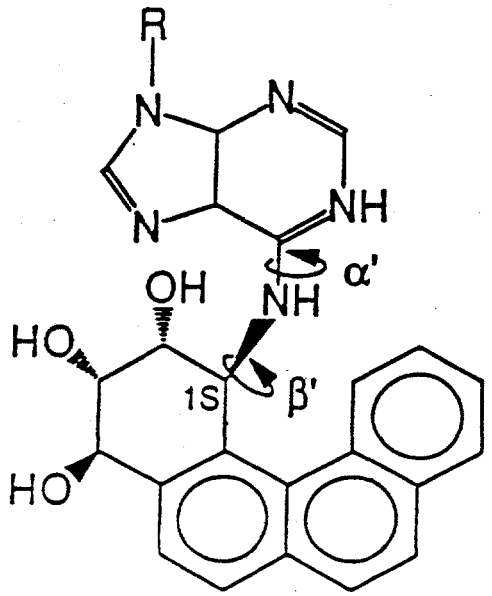

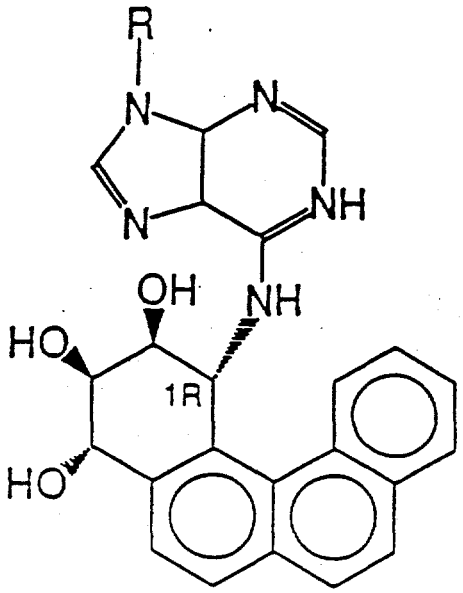

1*S* (-)-*trans-anti*-[BPh]-N^6-dA 1*R* (+)-*trans-anti*-[BPh]-N^6-dA

Figure 1 Structures of the 1*S* (-)-*trans-anti*- and 1*R* (+)-*trans-anti*-B[c]Ph-N^6-dA adducts. The torsion angles α' and β' that define the orientations of the B[c]Ph residues in oligonucleotide sequences are shown.

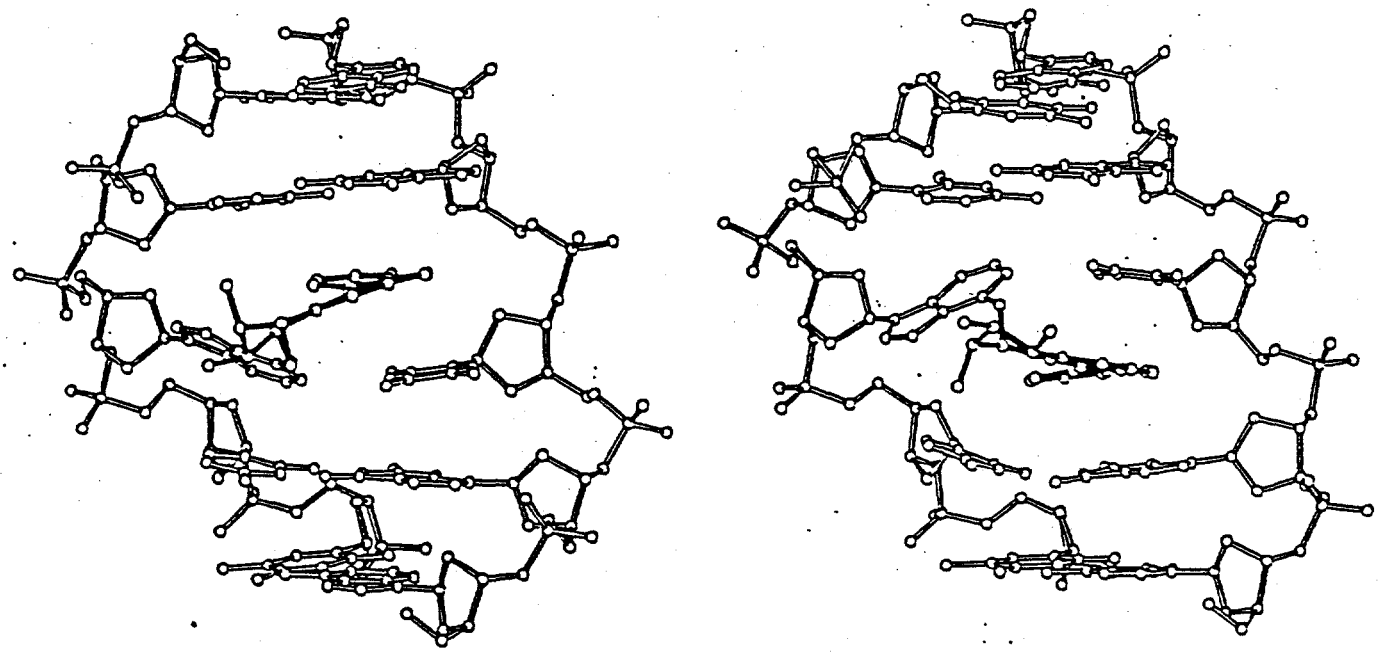

Figure 2 Conformations of the 1S (-)-*trans-anti*- and 1R (+)-*trans-anti*-B[c]Ph-N^6-dA lesions in the double-stranded oligonucleotide sequence (A* is the modified base) 5'-d(CTCCTCA*CTTCC).d(GGAAGTGAGAG). The 5'-ends of the modified strands are on the top in both cases, and the views are into the major groove, normal to the helix axis. Only the central five base pair segments are shown. Left: 1*R* (+)-*trans-anti*-B[c]Ph-N^6-dA, and Right: 1*S* (-)-*trans-anti*-B[c]Ph-N^6-dA.

In the (+)-*trans*-adduct, the B[c]Ph residue is intercalated on the 5'-side of the modified dA* residue, while in the (-)-*trans*-adduct it is intercalated on the 3'-side (From Cosman et al., 1993; 1995).

deoxyadenosine residue without disrupting the hydrogen bonding, whereas in *the* (-)-*trans-anti*-B[c]PhDE-N^6-dA adduct, the B[c]Ph ring intercalates on the 3'-side of the modified deoxyadenosine residue (Fig. 2).

In vivo, enzymes that repair, replicate, or degrade DNA may be sensitive to the conformational differences in PAH-diol-epoxide-DNA adducts. Mao et al. (Mao et al., 1993) have reported an example of the stereoselective inhibition of a pair of exonucleases (snake venom phosphodiesterase and spleen phosphodiesterase) by two stereochemically different PAH-DNA adducts which were derived from the pair of chiral diol epoxide enantiomers (+)-7R,8S,9S,10R and (-)-7S,8R,9R,10S of 7,8-dihydroxy-9,10-epoxy-7,8,9,10-tetrahydrobenzo[a]pyrene ((+)- and (-)-*anti*-BPDE, respectively). The relative rates of digestion by these two exonucleases were related to the conformations of the (+)- and (-)-*trans-anti-BPDE-*N^2-dG lesions as discussed in detail in the paper by Mao et al. (1993). In our previous DOE report (DOE/ER/60674-7, N.E. Geacintov, P.I.), we reported that the DNA polymerase kinetics *in vitro* did not reflect the orientations of the pyrenyl residues of these stereoisomers that have been deduced from structures of the NMR solution structures in double-stranded DNA (Cosman et al., 1992; de los Santos et al., 1992). However, this is not necessarily surprising, since the conformations of the pyrenyl residues at single-strand/double-strand junctions (as in a replication fork) can be quite different from those observed in double-stranded DNA (Cosman et al., 1995; Feng et al., 1997).

In this study, we tested the hypothesis that the *R* or *S* absolute configurations in adducts derived from the binding of *anti*-B[c]PhDE stereoisomers to deoxyadenosine residues in DNA influence the replication of DNA catalyzed *in vitro* by a typical enzyme, the Klenow fragment of Pol I (exonuclease-free). The results described in this report were obtained by Dr. Bin Li who received his Ph.D. degree from New York University in 1996.

The Klenow fragment (exonuclease-free) of *E. coli* DNA polymerase I was chosen for this work because X crystallography (Ollis et al., 1985) and DNA synthesis kinetic mechanism studies (Kuchta et al., 1987; Dahlberg and Benkovic, 1991; Carroll and Benkovic, 1990) have provided a wealth of information on this enzyme.

A quantitative gel assay was developed by Boosalis et al. (Boosalis et al., 1987) to measure the Michaelis-Menten kinetic parameters (V_{max} and K_m) for nucleotide insertion at any single site along a DNA template strand. This method has been used to study the DNA synthesis fidelity by quantitatively evaluating the parameters V_m, K_m, and the frequency of nucleotide incorporation (V_{max} / K_m) in a number of site-direct mutagenesis studies *in vitro* (Singer et al., 1989; 1990; Dosanjh et al., 1993; Shibutani et al., 1993).

We first review the principles, as well as the terminology associated with these kinds of DNA polymerase-catalyzed primer extension reactions in vitro.

2. DNA Polymerase Kinetics *in vitro*: Steady-State Michaelis-Menten Kinetics

In enzyme kinetics, the concept of the steady-state refers to the situation in which the concentrations of enzyme-bound intermediates, [E·S], remain constant. We briefly review the basics of steady-state Michaelis-Menten enzyme catalysis since we use this approach to study

the effects of the PAH lesions on the efficiency of DNA synthesis. The general Michaelis-Menten mechanism can be recalled as follows:

$$E + S \underset{k_{-1}}{\overset{k_1}{\rightleftharpoons}} [E{\cdot}S] \xrightarrow{k_{cat}} P \text{ (product)} \qquad (1)$$

where E is the enzyme, S is the substrate (in our case the deoxynucleotide triphosphates, dNTP, that are incorporated into the growing primer strands), [E·S] is the enzyme-bound intermediate, P is the product, and k_1, k_{-1}, k_{cat} are the rate constants. The well known steady-state solution for V, the velocity of the reaction is:

$$k_{cat}\,[E]_0\,[S] / (K_m + [S]) = V_{max}\,[S] / (K_m + [S]) \qquad (2)$$

where V is the rate of appearance of product P ($V = dP/dt$).

When $[S] \rightarrow \infty$, V tends toward a limiting value termed V_{max}, the maximum rate of reaction. $V_{max} = k_{cat}\,[E]_0$, where $[E]_0$ is the concentration of the enzyme.

We further define the Michaelis-Menten constant

$$K_m = (k_2 + k_{-1}) / k_1 \qquad (3)$$

When $k_{-1} >> k_2$, $K_m \approx k_{-1}/ k_1$, is very close to the dissociation constant of the complex ES. Equation (2) can be rearranged as follows:

$$S / V = S / V_{max} + K_m / V_{max} \qquad (4)$$

A plot of S/V as a function of S should yield a straight line (Hanes-Woolf plot) from which the parameters V_{max} and K_m can be determined from the slope and intercept, respectively.

Significance of k_{cat}: the catalytic rate constant.

The rate constant k_{cat} is related to the experimentally determined value of the maximum reaction velocity, V_{max}, by the relationship $V_{max} = k_{cat}\,[E]_0$. In the simple Michaelis-Menten mechanism in which there is only one enzyme-substrate complex ($V = k_{cat}\,[E{\cdot}S]$ and all binding steps are fast), k_{cat} is simply the first-order rate constant for the chemical conversion of ES → EP. For more complicated reaction, k_{cat} is a function of all of the first-order rate constants included in the reactions, and $1/k_{cat} = 1/k_2 + 1/k_3 + \cdots$ (Fersht 1985); in such cases, k_{cat} cannot be assigned to any particular process except when some simplifying features occur. For example, in reaction (1), when the dissociation of the EP complex is fast, k_{cat} is equal to k_2. But if the dissociation of the EP complex is slow, the reaction should be written as

$$E + S \underset{k_{-1}}{\overset{k_1}{\rightleftharpoons}} [E\cdot S] \xrightarrow{k_2} [E\cdot P] \xrightarrow{k_3} E + P \qquad (5)$$

with $k_{cat} = k_2 k_3 / (k_2 + k_3)$ or, alternatively, $1/k_{cat} = 1/k_2 + 1/k_3$. The rate constant k_3 for dissociation of the EP complex contributes to k_{cat}, and in the extreme case in which EP dissociation is far slower than the chemical steps (ES → EP), k_{cat} will be equal to the dissociation constant, k_3.

Significance of K_m.

Although it is only in the case of simple Michaelis-Menten mechanisms, or in similar cases, that $K_m = K_S$, (K_S is the true dissociation constant of the enzyme-substrate ES), K_m may be treated as an apparent dissociation constant of all enzyme-bound species: $K_m = [E][S] / \sum [E\cdot S]$, where $\sum [E\cdot S]$ is the sum of all of the bound enzyme species. For example, in the reaction (5), the apparent Michaelis constant, is $K_m = K_S k_3/(k_2 + k_3)$. If $k_3 >> k_2$ (step 2 is the rate-limiting step), $K_m \approx K_S$, which is very close to the true dissociation constant of ES complex. If $k_2 >> k_3$ (step 3 is the rate-limiting step), $K_m \approx K_S k_3/ k_2 < K_S$, which is smaller than K_S by a factor of k_3 / k_2.

The enzymatic steps leading to the extension of primer DNA from n to n+1 nucleotides can be described simply as follows:

$$[E\cdot DNA_n] + dNTP \underset{k_{-1}}{\overset{k_1}{\rightleftharpoons}} [E\cdot DNA_n\cdot dNTP] \xrightarrow{k_{cat}} E + DNA_{n+1} + PPi \qquad (6)$$

The insertion velocity, $V = k_{cat} [E\cdot DNA_n\cdot dNTP]$, where $[E\cdot DNA_n\cdot dNTP]$ is the concentration of the enzyme-DNA-dNTP ternary complex, and k_{cat} is the rate constant, and V should obey Michaelis-Menten kinetics $V = V_{max} [dNTP] / (K_m + [dNTP])$. The Michaelis constant $K_m = (k_{-1} + k_{cat}) / k_1 \approx k_{-1} / k_1$, is very close to the dissociation constant of the substrate dNTP from the DNA-polymerase-dNTP ternary complex. Under these conditions, $V_{max} = k_{cat} [E\cdot DNA_n]_t$, where $[E\cdot DNA_n]_t$ is the total concentration of enzyme-DNA and enzyme-DNA-dNTP complex involved in the reaction.

V_{max}/K_m, is called the frequency factor or the insertion specificity, f, which indicates the efficiency with which each nucleotide dNTP is inserted by a polymerase. As will be demonstrated later, the study of apparent Michaelis-Menten parameters, K_m, V_{max}, k_{cat} and f provides powerful insights into the mechanisms of polymerase-catalyzed DNA synthesis and indicates how the function of a typical polymerase is affected by a B[c]PhDE-N^6-dA lesion positioned site-specifically in an oligonucleotide template strand.

3. Materials and Methods

3.1 Synthesis and Characterization of Site-Specific and Stereospecific B[c]PhDE - N^6-dA Modified Oligonucleotides

Racemic *anti*-B[c]PhDE was synthesized according to published procedures (Misra and Amin, 1990). A 1 mM stock solution of anti-B[c]PhDE in THF was prepared and used in the modification of oligonucleotides. The 19 base-long oligonucleotide 5'-d(TCTCACCCTCCTTTCCTCT) was purchased from Midland Certified Reagent Co. (Midland, TX) and was further purified by HPLC prior to the modification of the oligonucleotides with *anti*-B[c]PhDE. The synthesis of the site-specifically modified and stereochemically defined oligonucleotides has been fully described in the paper by Laryea et al. (1995), and therefore will not be repeated here.

3.2. Polymerase-catalyzed DNA Synthesis Using Site-specific and Stereospecific trans-anti-B[c]PhDE-N^6-dA Modified Oligonucleotide As Templates

3.2.1 Materials. The oligodeoxyribonucleotides 5'-d(TCTCACCCTCCTTTCCTCT) (19mer), 5'-d(AGAGGAAAGGAGG) (13mer), 5'-d(AGAGGAAAGGAGGG) (14mer), and 5'-d(AGAGGAAAGGAGGGT) (15mer) were purchased form the Midland Certified Reagent Co. (Midland, TX) and were further purified by HPLC. Exonuclease-free Klenow fragment of *E. coli* polymerase I and T4 polynucleotide kinase were obtained from the United State Biochemical Corp. (Cleveland, OH). [γ-^{32}P] ATP was purchased from New England Nuclear (Boston, MA). Unmodified and B[c]PhDE-modified 19-mer templates (10 pmol) were labeled with ^{32}P at the 5' terminus using the T4 polynucleotide kinase and then subjected to 20% polyacrylamide gel electrophoresis in the presence of 7 M urea to check for impurities.

3.2.2 Primer-Template Annealing. The 19-mer template containing a single dA residue, or a B[c]PhDE-modified dA residue, was annealed with ^{32}P-labeled primer (13-mer, 14-mer, or 15-mer) in a buffer of 50 mM Tris-HCl (pH 8.0), 5 mM $MgCl_2$, and 2 mM β-mercaptoethanol. This primer-template solution (100 nM) was incubated at 85 ^{0}C for 2 min and then cooled slowly to 22 ^{0}C.

3.2.3 General Method of DNA Polymerase Reaction. Reactions for determining V_{max} and K_m were begun by mixing equal volumes (5 μL) of solution A containing primer-template-enzyme complex and solution B containing one dNTP as substrate as described by Randall et al. (1987). Solution A was made by adding 1 μL of exonuclease free Klenow fragment of Pol I to 44 μL of the original primer-template annealing solution. Solution B contained 50 mM Tris-HCl (pH 8.0), 5 mM $MgCl_2$, 2 mM β-mercaptoethanol and various concentrations of dNTPs. The polymerization reaction was allowed to proceed at 22 ^{0}C for different time intervals and was terminated by adding 20 μL of 20 mM EDTA in 95% formamide. For insertion before the lesion (sequence 13/19mer), or extension after the lesion (sequence 15/19mer), the normal substrate dGTP at concentration ranges from 0.01 μM to 50 μM was added. For insertion opposite to the lesion (sequence 14/19mer), the substrate dTTP was added at concentration ranges from 10 μM to 5 mM. Samples of this mixture were then subjected to 20% polyacrylamide gel electrophoresis.

The reaction conditions for the time course experiments were the same as above except that the reaction times varied between 0 and 20 min. The concentration of substrate dGTP in the

insertion before the lesion or extension after the lesion was 0.5 μM or 2 μM, and the substrate dTTP concentration in the insertion opposite to the lesion was 2 μM or 500 μM in the case of the unmodified, or B[c]PhDE modified templates, respectively.

3.2.4 Calculation of V_{max}, K_m, and the Frequency of Incorporation, f. Electrophoretic gel bands were quantified by autoradiography. The spatial distribution of the radioactivity on the gels was measured with a Phosphor Imager Model GS-250 (BioRad, Hercules, CA). The calculations of the V_{max}, K_m , and f values, were as described by Mendelman et al. (1989). The velocity of nucleotide incorporation upon extending the primer (band 0), or by inserting one single nucleotide into the primer (band 1), are expressed in terms of the integrated gel band intensities, after a reaction time interval Δt, as $V_{01} = (100\ I_1) / (\ I_0 + 0.5\ I_1)\Delta t$. Typically, no more than 20% of total primer was used in these reactions in order to ensure linearity. V_{max} and K_m were obtained from Hanes-Woolf plots and were averaged from at least two independent experiments.

4. Results

4.1 Overview of Experimental Approach.

In this work, we have studied the steady-state Michaelis-Menten kinetics of DNA synthesis using site-specifically modified and stereochemically defined oligonucleotide templates containing single B[c]PhDE-N^6-dA lesions, and primers of different lengths. Single dNTP substrates (S) were used in all cases. Three different types of reaction were studied using three different template/primer complexes as defined in Figure 3.

Insertion before the lesion:

dGTP
↓ GGAGGAAAGGAGA-5' primer
5'-dTCTCA*C C CTCC TTT CCTCT-3' template
(Sequence 13 / 19mer)

Insertion opposite the lesion:

dTTP
↓ G GGAGGAAAGGAGA-5' primer
5'-dTCTCA*C C CTCC TTT CCTCT-3' template
(Sequence 14 / 19mer)

Extension after the lesion:

dGTP
↓T G GGAGGAAAGGAGA-5' primer
5'-dTCTCA*C C CTCC TTT CCTCT-3' template
(Sequence 15 / 19mer)

Figure 3. Sequences of the three template-primer complexes used in this study

In each experiment, the kinetics of incorporation of a single base dNTP (either dGTP or dTTP), opposite the template with a site-specific and stereospecific (+)-*trans* or (-)-*trans-anti*-B[c]PhDE-N^6-dA lesion (designated as **A***) was studied. By controlling the primer extension by adding only one single base to the primer strand at a time (the natural base in each case), we were able to systematically test the effects of the (+)-trans and (-)-*trans-anti*-B[c]PhDE lesions on nucleotide incorporation just before the lesion (sequence 13/19mer), opposite the lesion (sequence 14/19mer), and extension of the primer after the lesion (sequence 15/19mer).

4.2 Hypothesis Tested.

The hypothesis tested in these experiments was that the stereochemical characteristics of the B[c]Ph residues covalently bound to deoxyadenosine residues in DNA impeded the normal synthesis of DNA (primer extension) in a stereospecific manner. Specifically, possible effects of adduct orientation, which is dependent on the *1R* or *1S* absolute configuration at the B[c]PhDE-N^6-dA linkage site (Cosman et al., 1995b), on the Michaelis-Menten parameters were evaluated just before the lesion, opposite the lesion, and after the lesion.

If we assume that in the model replication fork sequence 13/19mer, 14/19mer and 15/19mer, similar adduct orientations are maintained as in the full duplex (Fig. 2) in which (+)-*trans-anti*-B[c]Ph residue points to the 5'-end of the modified strand and in the (-)-*trans*-adducts the B[c]Ph residue points towards the 3'-end, then the following effects of the B[c]PhDE lesions on DNA synthesis are predicted:

1. In the case of the 13/19mer sequence, with the bulky (-)-*trans*-B[c]PhDE residue predicted to be positioned on the 3'-side of the modified dA residue (Cosman et al., 1995b), DNA synthesis just before the lesion is expected to be more hindered in the case of the (-)-*trans*-adduct than in the case of the (+)-*trans*-adduct.
2. In the case of the 15/19mer, with the (+)-*trans*-B[c]PhDE residue being located on the 5'-side of the modified dA residue (Cosman et al., 1993), dNTP insertion into the primer just after the lesion using the dC residue flanking the lesion on the 5'-side, should be more inhibited in the case of the (+)-*trans* than in the case of the (-)-*trans* adduct.
3. Insertion of the normal dTTP into the primer using the B[c]Ph-modified dA* residue as a template (the 14/19-mer in Fig. 3) should depend only to a lesser extent on the orientation of the B[c]Ph residue, and should be severely hindered in both cases since normal base pairing between the dTTP and dA* is compromised by the presence of the bulky B[c]Ph residue.

These hypotheses were tested by studying the dependence of the kinetic DNA synthesis parameters V_{max}, K_m, V_m/K_m , on DNA adduct stereochemistry.

4.3 DNA Synthesis Kinetics

All of the steady-state kinetic studies of nucleotide incorporation presented in this work

were carried out using an exonuclease-free Klenow fragment of *E. coli* DNA polymerase I. The exo$^-$ Klenow fragment was used because the exonuclease activity of the wild-type enzyme would have excised any misincorporated nucleotide before further elongation occurred using its proofreading mechanism (Eger et al., 1991). In such reactions with the wild-type Klenow fragment, the primer strand can be degraded if the correct dNTP is not supplied during the incubations; thus, only primer degradation rather than primer elongation events were observed by Christner et al. (1994) in DNA synthesis experiments using oligonucleotide templates with single BPDE-N^6-dA lesions.

4.3.1 Kinetics of Insertion Before the Lesion

The kinetic parameters were determined using the polyacrylamide gel polymerase fidelity assay used by Randall et al. (1987) and by Boosalis et al. (1987). This method has been very useful for the quantitation of base incorporation in site-directed mutagenesis studies *in vitro* (Singer et al., 1989; 1990; Dosanjh, 1991; Shibutani, 1993). In order to satisfy the requirements for steady-state kinetics, the appropriate polymerase reaction conditions (enzyme concentration, reaction times) should be determined which result in a linear increase in the amount of reaction products as a function of increasing time of reaction; furthermore, less than 20% of the input primer should undergo reaction (Mendelman et al., 1989; 1990). Time course experiments were required to determine the linear range of band intensity versus reaction time for each primer/template.

The evolution in time of each band intensity as a function of reaction time is illustrated in Figures 4 and 5. It should be noted that only the substrate dGTP was present in these reactions in order to control primer extension one base at a time. The concentration of dGTP was 1 μM for the unmodified template case, and 2 μM for the two modified templates. The incorporation of dGTP before the lesion and opposite a C residue on the template strand, is faster in the case of the (+)-*trans*-adduct than in the case of the (-)-*trans*-adduct, but is slower than in the case of the unmodified template strand.

Under our experimental conditions using the 13/19-mer sequence, following incorporation of the correct G just before the lesion, the enzyme can also misincorporate a G opposite the lesion, thus forming a G·A mismatch; this was evident from faint G·A bands above the G·C band which were observed in the original gels (these are not visible in Figure 4). The primer strands with mismatched G·A termini can be further extended beyond the lesion incorporating G opposite the next base C on the template strand in the case of the unmodified template as is evident in panel (A) in Fig. 4. In panels (B) and (C) in Fig. 4, showing primer extension with templates containing single (+)-*trans*-B[c]PhDE-N^6-dA and (-)-*trans*-B[c]PhDE-N^6-dA lesions, primer extension essentially stopped after insertion of the single G just before the lesion. However, minor amounts of G were also incorporated opposite the (+)-*trans*-modified template, as was evident from the corresponding faint bands in the original gels (these are not visible in panel (B) in Fig. 4, however). Analogous bands are not visible in the original gel in the case of the (-)-*trans* adducted template strand. These observations suggest that the (+)-*trans-anti*-B[c]PhDE-N^6-dA lesion is somewhat more easily

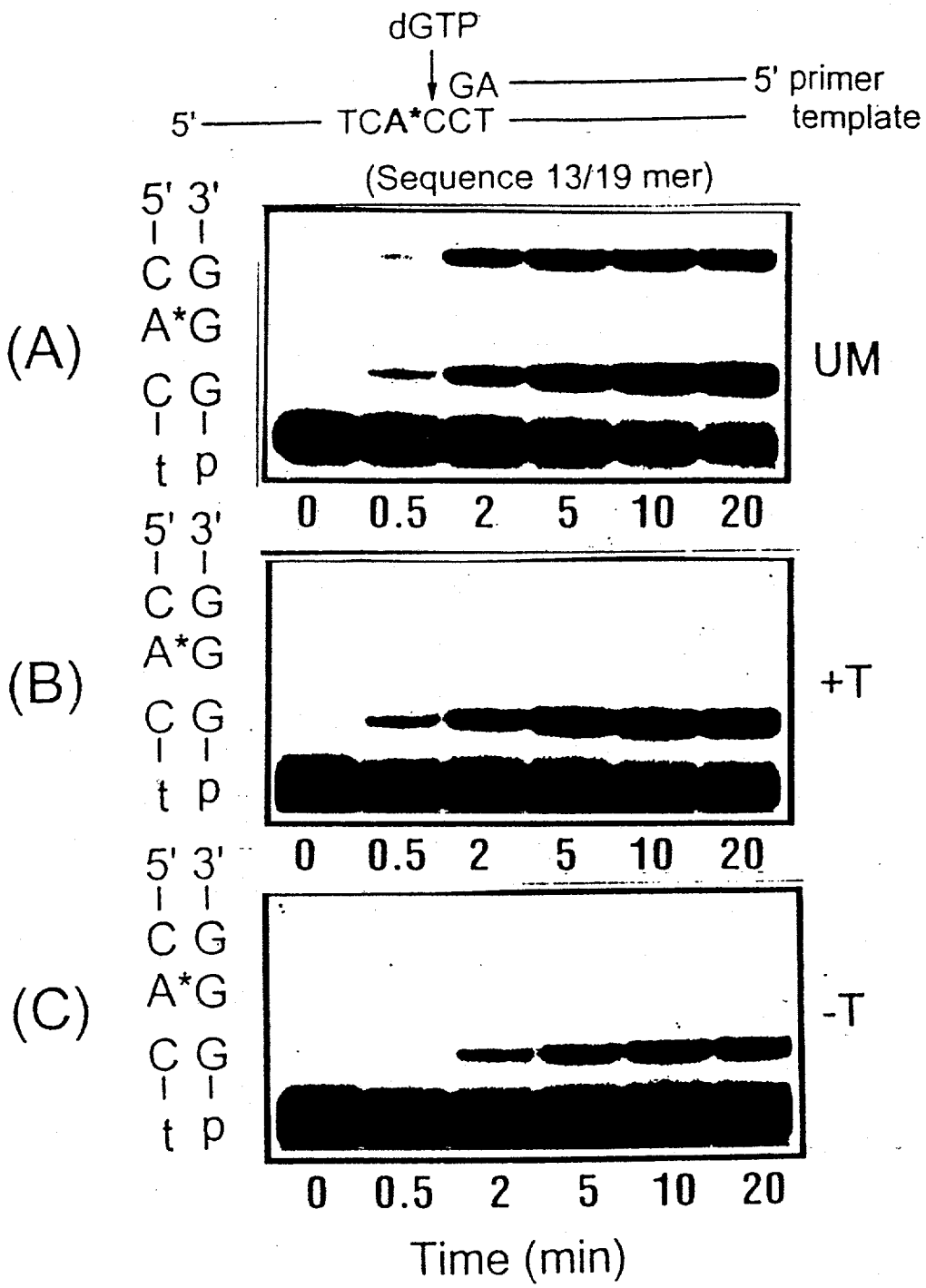

Figure 4 Gel autoradiogram showing the insertion of dGTP before the lesion site as a function of reaction time. Only dGTP is present as substrate in the reaction mix. [primer/template] = 100 nM, [enzyme] = 3.4 nM.

(A) unmodified oligonucleotide (UM) as template, [dGTP] = 0.5 μM.

(B) (+)-trans-B[c]PhDE-dA modified oligonucleotide (+T) as template, [dGTP] = 2 μM.

(C) (-)-trans-B[c]PhDE-dA modified oligonucleotide (-T) as template, [dGTP] = 2 μM.

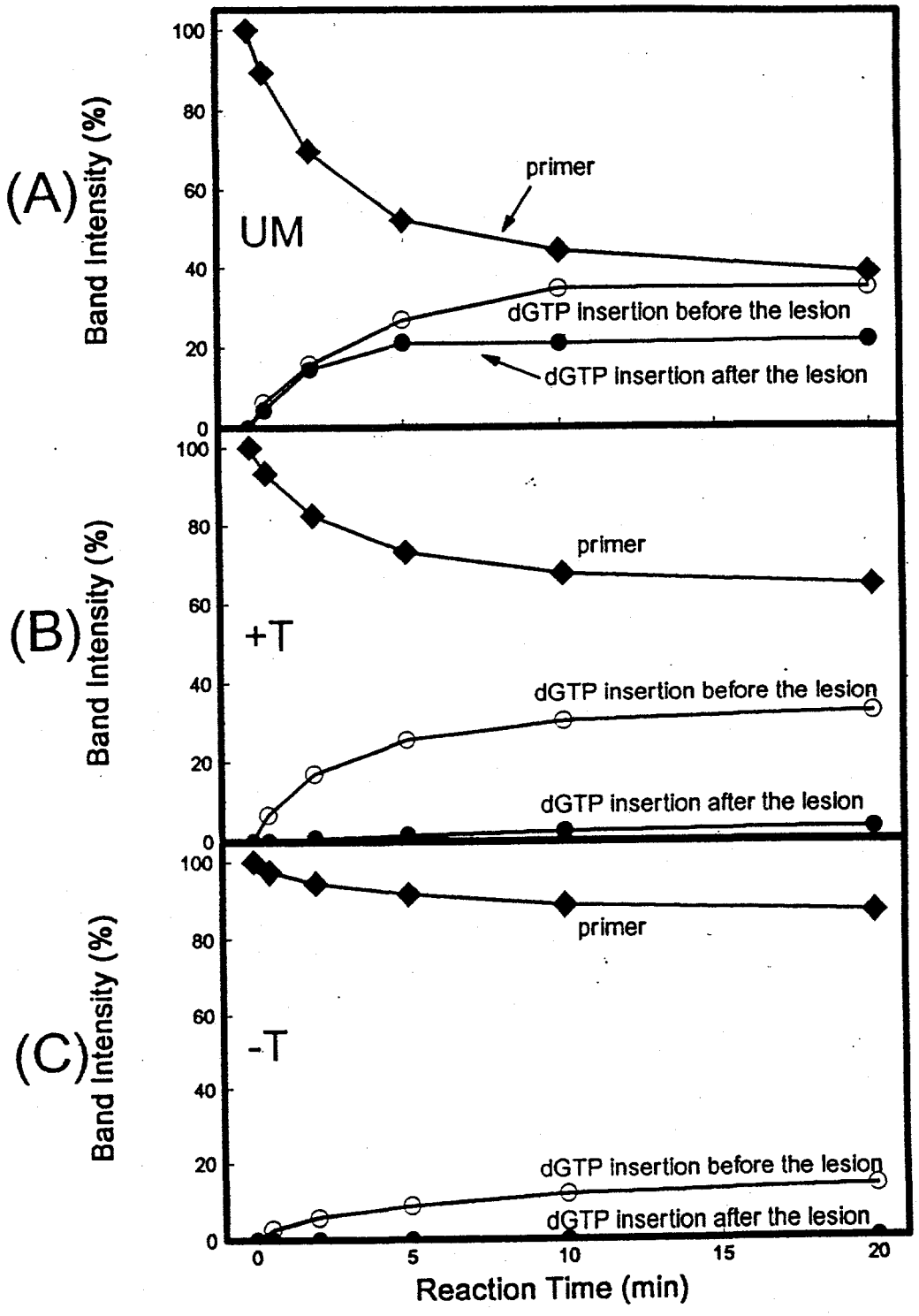

Figure 5 **Relative band intensities as a function of time for insertion of dGTP before the lesion. The intensity value for each band is expressed as a percentage of the total intensity, summed over all bands shown in the gels depicted in Figure 4. The plots in panels (A), (B), and (C) correspond to panels (A), (B), and (C) shown in Figure 4.**

bypassed than the (-)-*trans*-B[c]PhDE-N^6-dA lesion under the experimental conditions of our experiment.

In Figure 5, the band intensities are expressed as a percentage of the total integrated intensities of all of the bands, including the original primer band, to show the relative intensity changes with reaction times of up to Δt = 20 min. It shows that the Δt = 90 sec time point represents a suitable reaction time for the unmodified and the modified templates since the band intensities increase approximately linearly with time.

With each template, the velocity of dGTP incorporation before the lesion site was measured at various substrate concentrations. Figure 6 is an example of electrophoretic bands observed as a function of different substrate concentrations (dGTP) varying from 0.02 μM to 5 μM, and from 0.1 μM to 20 μM for the (+-)-*trans*- and (-)-*trans*-B[c]PhDE-modified template strands, respectively. The higher intensity of the G·C band (constituting the 3'-primer/5'-template junction base pair) in the in (+)-*trans*-adduct case (Figure 4 (A)) again indicates that dGTP insertion before the lesion is easier in the case of the (+)-*trans* adduct than in the case of the (-)-*trans*-adduct.

In order to measure the velocity (V) at each substrate concentration, we simply use $V = 100\, I_1 / (I_1 + 0.5I_0)\Delta t$ (see the experimental procedure), where I_1 is the intensity of the extended primer band, and I_0 is the intensity of the unelongated primer band. The plot of V versus [dNTP] shows typical saturation kinetics for each template (Figure 7), and this relationship conforms to the steady-state Michaelis-Menten kinetics. Having evaluated V versus [S] in this manner, we then determine V_{max} and K_m from a least-squares fit to a straight line in a Hanes-Woolf plot, [S]/V versus [S]. Figure 8 shows some typical Hanes-Woolf plots for each of the three types of templates studied by us. V_{max} is the slope of the straight line and K_m is the X-axis intercept. The average values of V_{max} and K_m were obtained from at least two independent determinations and are summarized in Table 1.

For insertion of dGTP before the lesion site, V_{max} is 34.2 min^{-1} for the unmodified, and only 4-12 min^{-1} for the modified templates. The V_{max} of the (+)-*trans* adduct (11 min^{-1}) is about 3-fold higher than that of the (-)-*trans*-adducts (3.9 min^{-1}). This order of reaction velocities is consistent with the known stereochemical properties of the *anti*-B[c]PhDE-N^6-dA adducts: the (+)-*trans*-B[c]Ph residue if we assume that it is oriented towards the 5'-side and that the (-)-*trans*-B[c]Ph residue points towards the 3'-side of the modified deoxyadenosine residue on the template strand (Fig. 2).

The values of K_m are 0.12 μM for the unmodified, 0.24 μM for the (+)-*trans*- and 0.64 μM for the (-)-*trans*-B[c]PhDE-modified template strands. These results indicate that the binding affinities of the substrate is at least 2-fold smaller for the (-)-*trans* than for the (+)-*trans*-B[c]Ph adduct. The overall efficiency of dGTP insertion before the lesion, as expressed by the frequency factor f ($f = V_m/K_m$) for the (+)-trans-adduct is 6 times lower than for the unmodified template strand, but 7 times higher than in the case of the (-)-*trans*-B[c]PhDE-modified template strand. Thus, the efficiency of nucleotide incorporation just before the lesion site depends strongly on the stereochemistry of the B[c]PhDE adducts.

The 7-fold higher efficiency of nucleotide incorporation into the primer strand using the base C before the (+)-*trans*-B[c]Ph-N^6-dA lesion as a template as compared to the (-)-*trans*-B[c]Ph-N^6-dA lesion, can be attributed to the higher insertion velocity (V_{max} is 3-fold higher)

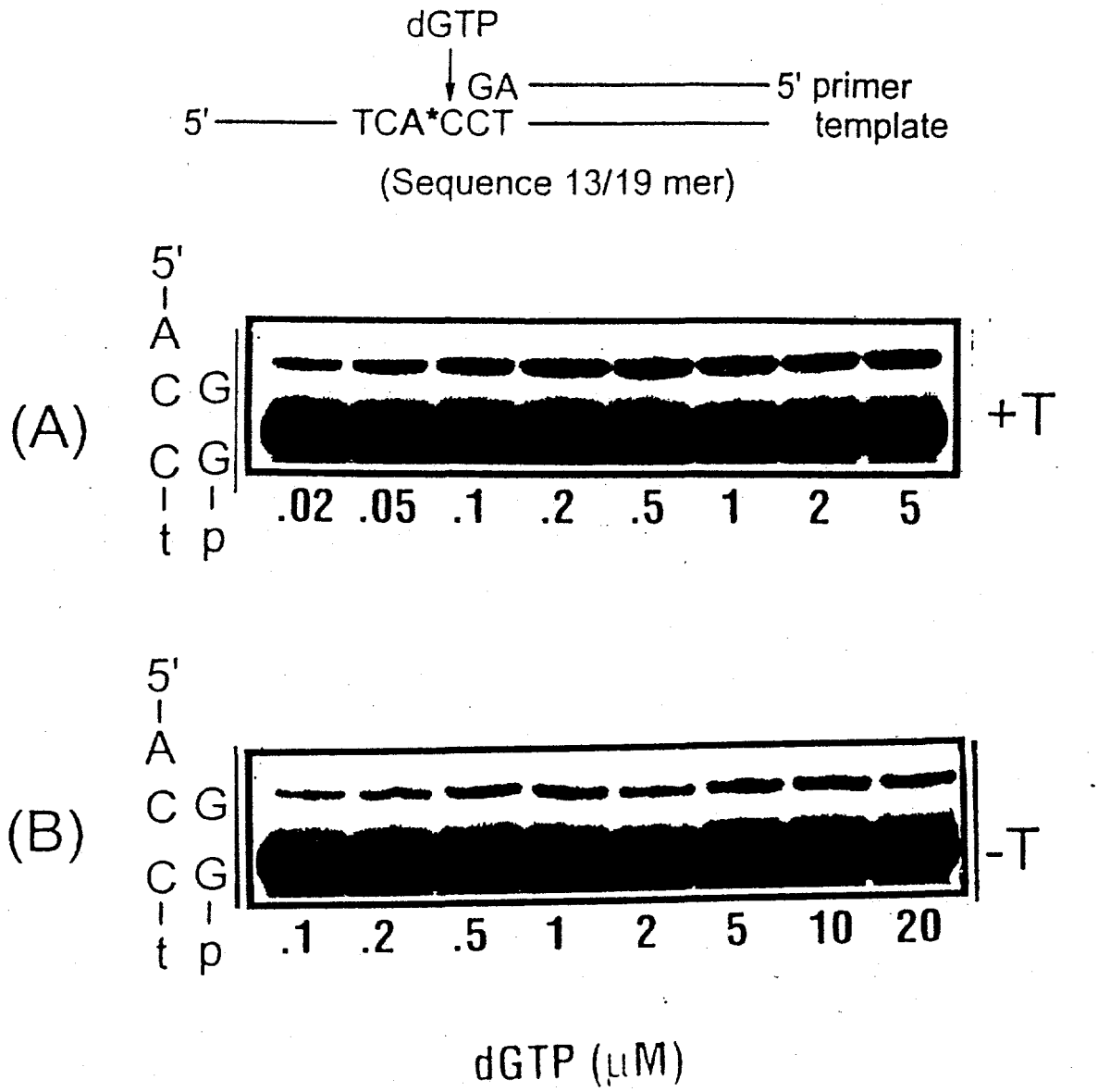

Figure 6 Gel autoradiogram for insertion of dGTP before the lesion site showing band intensities as a function of dGTP substrate concentration

(A) (+)-trans-B[c]PhDE-dA modified oligonucleotide as template, [template/primer] = 100 nM, [enzyme] = 3.4 nM, reaction time = 90 sec.

(B) (-)-trans-B[c]PhDE-dA modified oligonucleotide as template, [template/primer] = 100 nM, [enzyme] = 3.4 nM, reaction time = 90 sec.

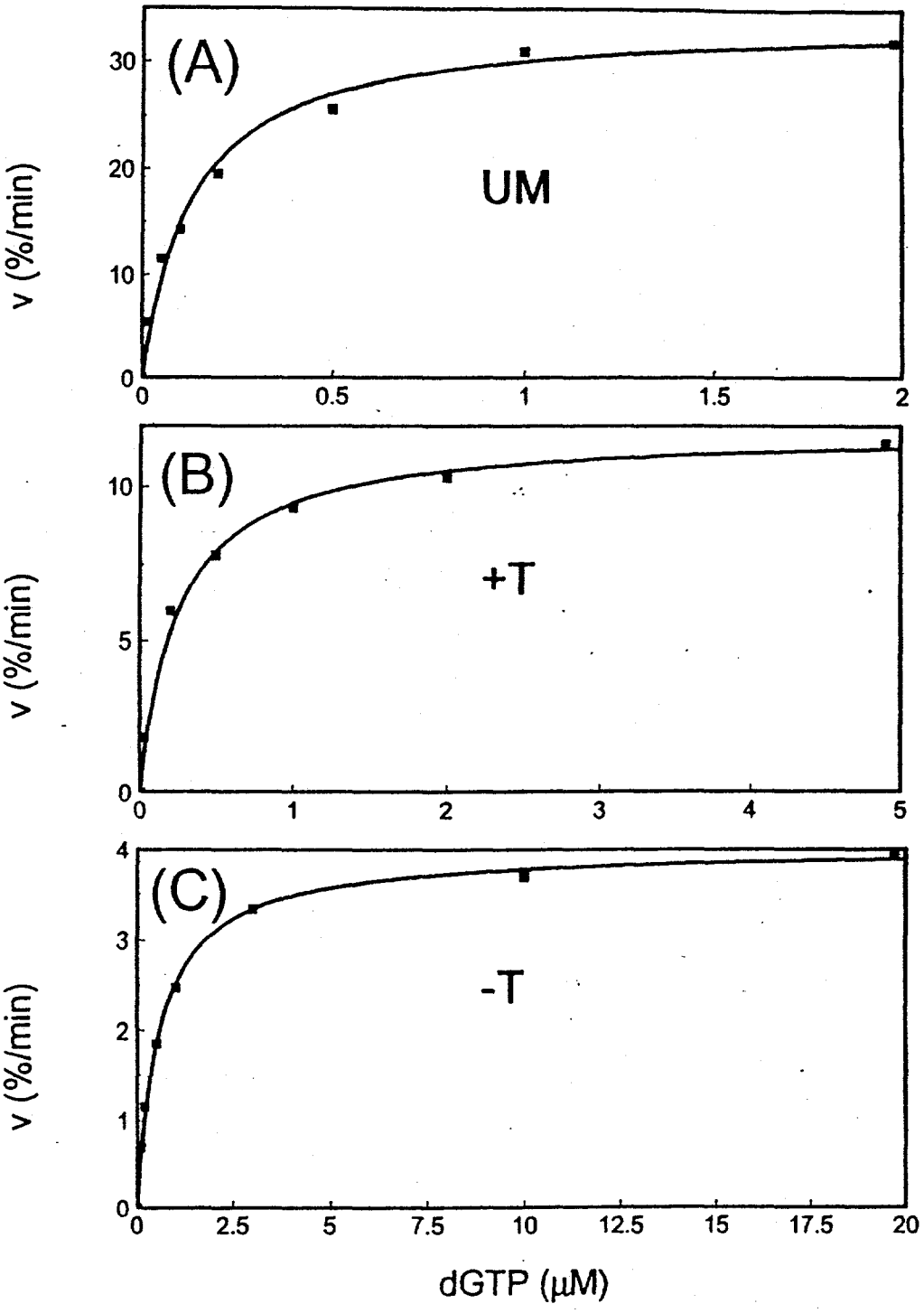

Figure 7. Insertion velocity (V) of dGTP before the lesion site as a function of dGTP substrate concentration, calculated from the band intensities in Figure 6, using the relation $V = 100\ I_0 / [(0.5\ I_1 + I_0)\Delta t]$. (A) Unmodified oligonucleotide template, (B) (+)-*trans-anti*-B[c]PhDE adducted template strand, (C) (-)-*trans-anti*-B[c]PhDE adducted template strand.

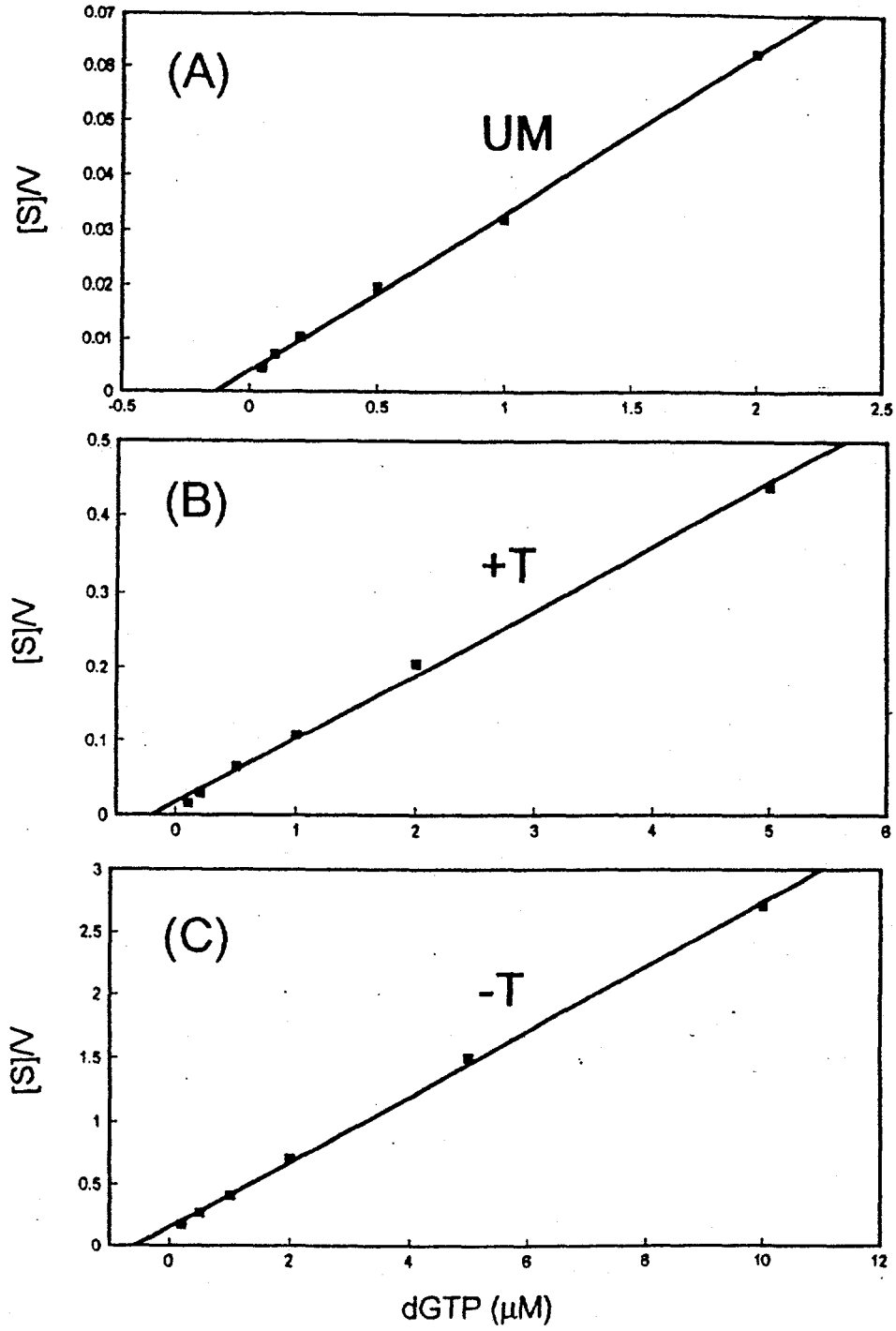

Figure 8 Hanes-Woolf plots for determining K_m and V_{max} for insertion of dGTP before the lesion site

(A) unmodified oligonucleotide template

(B) (+)-trans-B[c]PhDE adducted template

(C) (-)-trans-B[c]PhDE adducted template

and to a higher substrate binding affinity (K_m is 2.3-fold smaller).

4.3.2 Kinetics of Insertion Opposite the Lesion.

In this experiment, only dTTP is added to the reaction mixture since dT is the complementary base to the two lesions, the *trans*-B[c]Ph-N^6-dA residues, or the unmodified dA residue in the 14/19 mer (Fig. 3). Time course experiments were done to determine the appropriate reaction time and the amounts of enzyme (Fig. 9). The concentrations of dTTP for unmodified template was 2 μM, and was 500 μM in the case of the (+)-*trans* or the (-)-*trans-anti*-B[c]Ph-N^6-dA adducts. There is a large difference in the amount of dNTP incorporation opposite the lesion between the unmodified and the B[c]PhDE-modified template strands. As illustrated in Fig. 9(A) and Fig. 9(B), even with the lower dTTP concentration, the intensities of the T·A band are much higher in the case of the unmodified than for the (+)-*trans*- and (-)-*trans*-B[c]PhDE-modified templates.

trans-trans The Michaelis-Menten parameters were determined from the data in Fig. 10 and the plots in Fig. 11. The V_{max} values were found to be 2.5 min^{-1}, 1.3 min^{-1}, and 0.72 min^{-1} with K_m values of 0.07 μM, 15 μM, and 220 μM for the unmodified template, (+)trans-, and (-)-trans-B[c]PhDE-modified template strands, respectively. The frequency factor ($f = V_{max}/K_m$) of dGTP insertion opposite the lesion site dA* for the unmodified template is at least 500 times larger than for the B[c]PhDE-modified templates. This can be attributed to large reductions in the substrate binding affinities (higher K_m values) due to the bulky B[c]PhDE residues which destabilize the enzyme-DNA-substrate ternary complexes. The insertion of dTTP opposite the lesion is relatively easier in the case of the (+)-*trans*- than in the case of the (-)-*trans-anti*-B[c]PhDE-modified template strands (Table 1). This indicates that the (-)-*trans* lesion blocks the primer elongation more effectively than the (+)-*trans-anti*-B[c]Ph-N^6-dA lesion.

4.3.3 Kinetics of extension after the lesion

The kinetics of incorporation into the primer strand of dGTP, opposite to the dC base on the template strand which flanks the trans-anti-B[c]PhDE-N^6-dA lesions, are depicted in Figs. 12 and 13. The band due to the primer extended by one base is already apparent even after the shortest reaction time of 0.5 min (Fig. 12, panel A). It is evident that the rate of incorporation in the case of the template with the (-)-*trans-anti*-B[c]PhDE-N^6-dA lesion is significantly greater than in the case of the template with the (+)-*trans-anti*-B[c]PhDE-N^6-dA adduct. This is evident from the greater intensity of the extended primer band in the case of the (-)-*anti*-B[c]PhDE-modified template (panel C in Fig. 12) than in the case of the (+)-*anti*-B[c]PhDE-modified template (panel B).

The Hanes-Woolf plots, [S]/V as a function of dGTP, are depicted for the three different types of 15/19-mer primer/template complexes in Fig. 14, and the values of V_{max} and K_m are summarized in Table 1. The rate of extension is almost 8 times higher for the (-)-*trans*-B[c]PhDE-modified (V_{max} = 20 min^{-1}) than for the (+)-*trans*-B[c]PhDE-modified template (V_{max} = 2.4 min^{-1}). The values of the frequency factors (f) is also greater for the

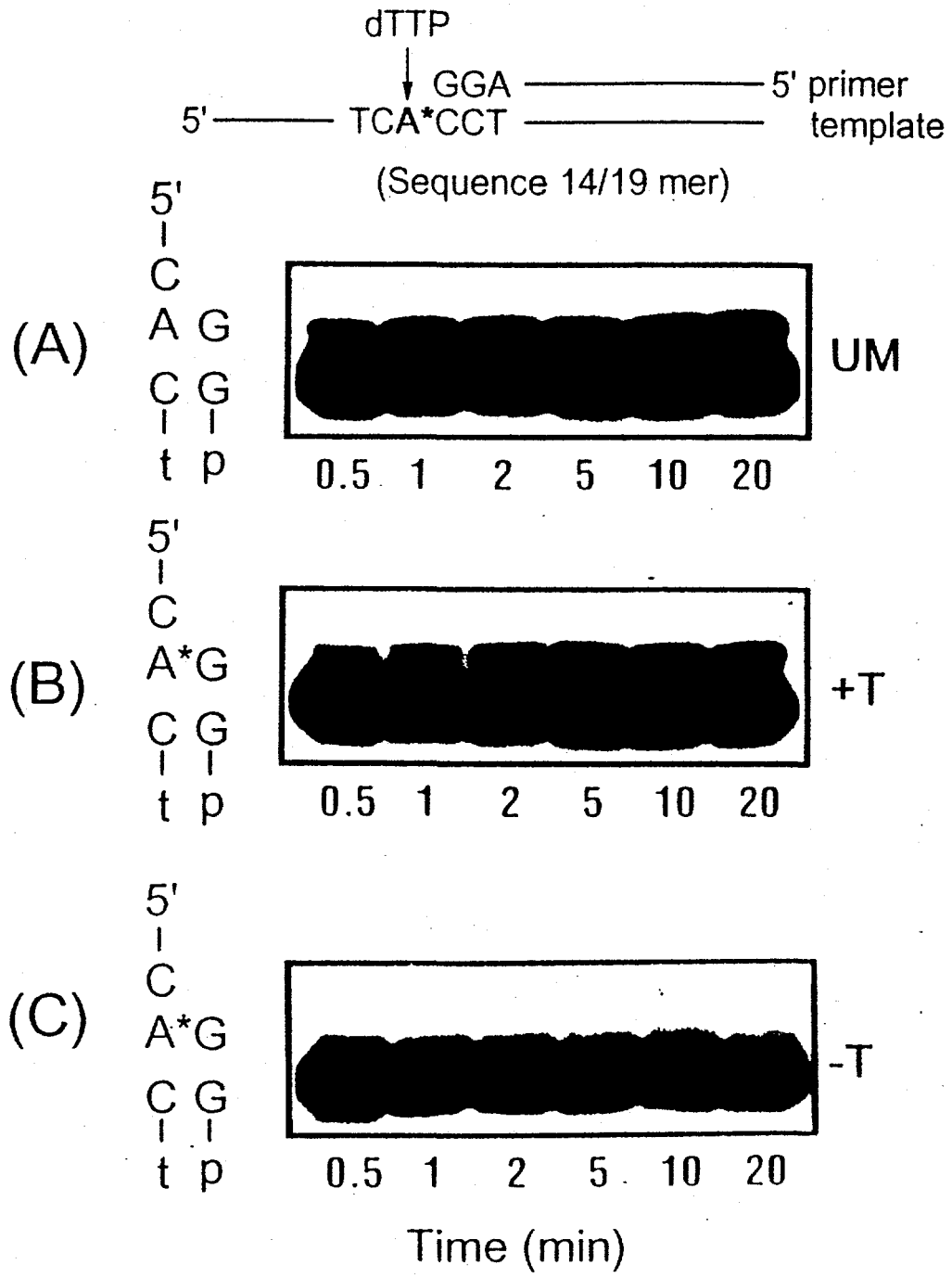

Figure 9 (a) Gel autoradiogram showing the insertion of dTTP opposite the lesion site as a function of reaction time. Only dTTP is present as the substrate in the reaction mix, [template/primer] = 100 nM, [enzyme] = 6.8 nM.

(A) unmodified oligonucleotide template, [dTTP] = 1.5 μM.

(B) (+)-trans-B[c]PhDE-dA modified oligonucleotide template, [dTTP] = 500 μM.

(C) (-)-trans-B[c]PhDE-dA modified oligonucleotide template, [dTTP] = 500 μM.

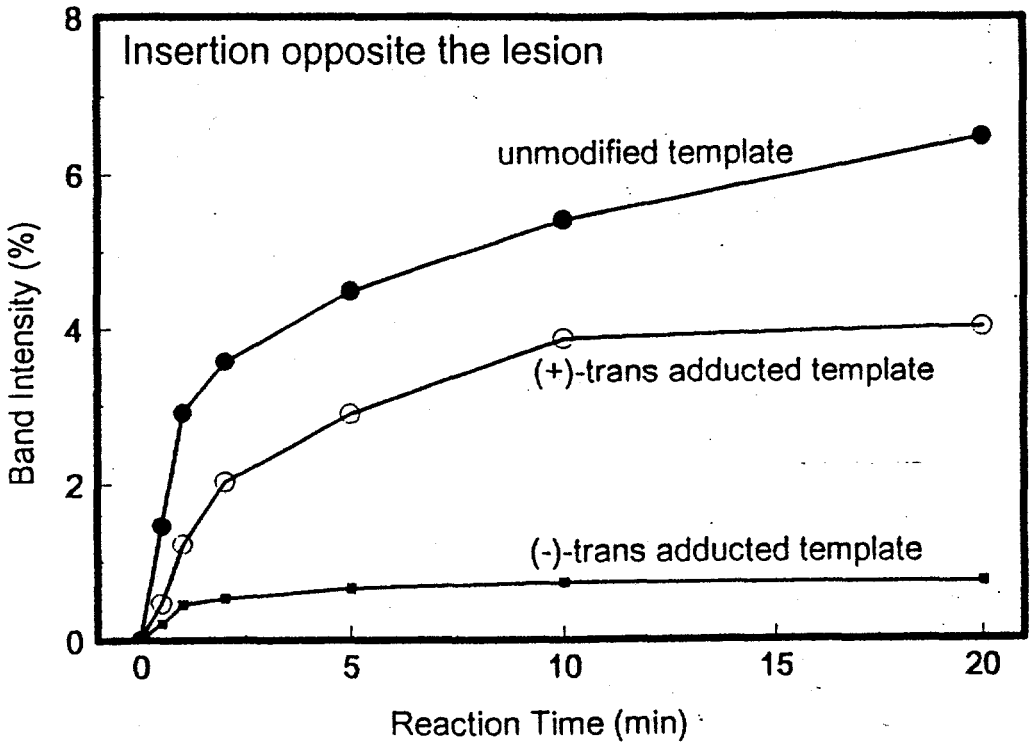

Figure 9 (b) Relative band intensities of extended primer as a function of reaction time for the insertion of dTTP opposite the lesion site, observed in Figure 9(a). The intensity values for each band are expressed as a percentage of the overall band intensities as defined in the legend to Figure 7.

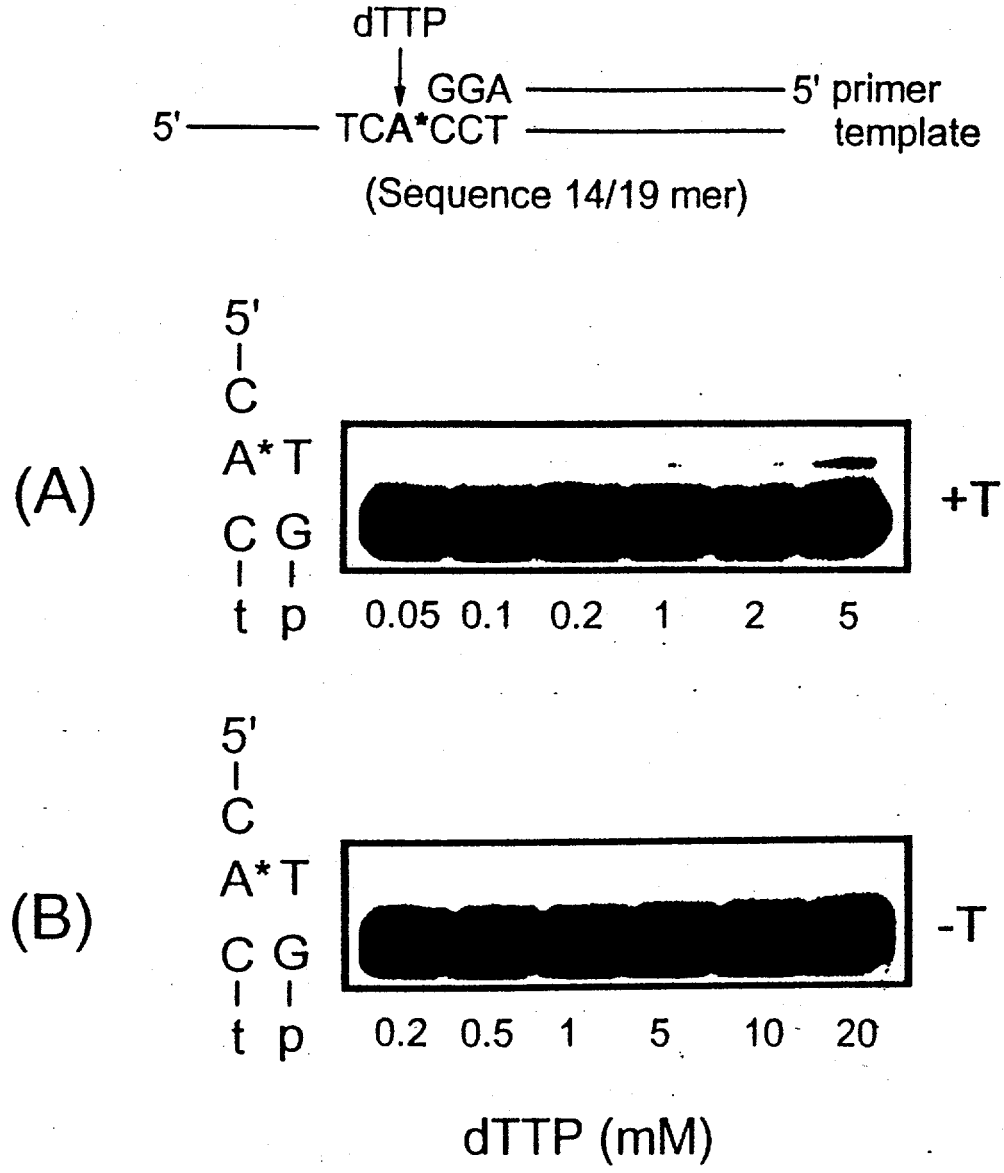

Figure 10 Gel autoradiogram for insertion of dTTP opposite the lesion site showing band intensities as a function of the dTTP substrate concentration

(A) (+)-trans-B[c]PhDE-dA modified oligonucleotide as template, [template/primer] = 100 nM, [enzyme] = 6.8 nM, reaction time = 90 sec.

(B) (-)-trans-B[c]PhDE-dA modified oligonucleotide as template, [template/primer] = 100 nM, [enzyme] = 6.8 nM, reaction time = 90 sec.

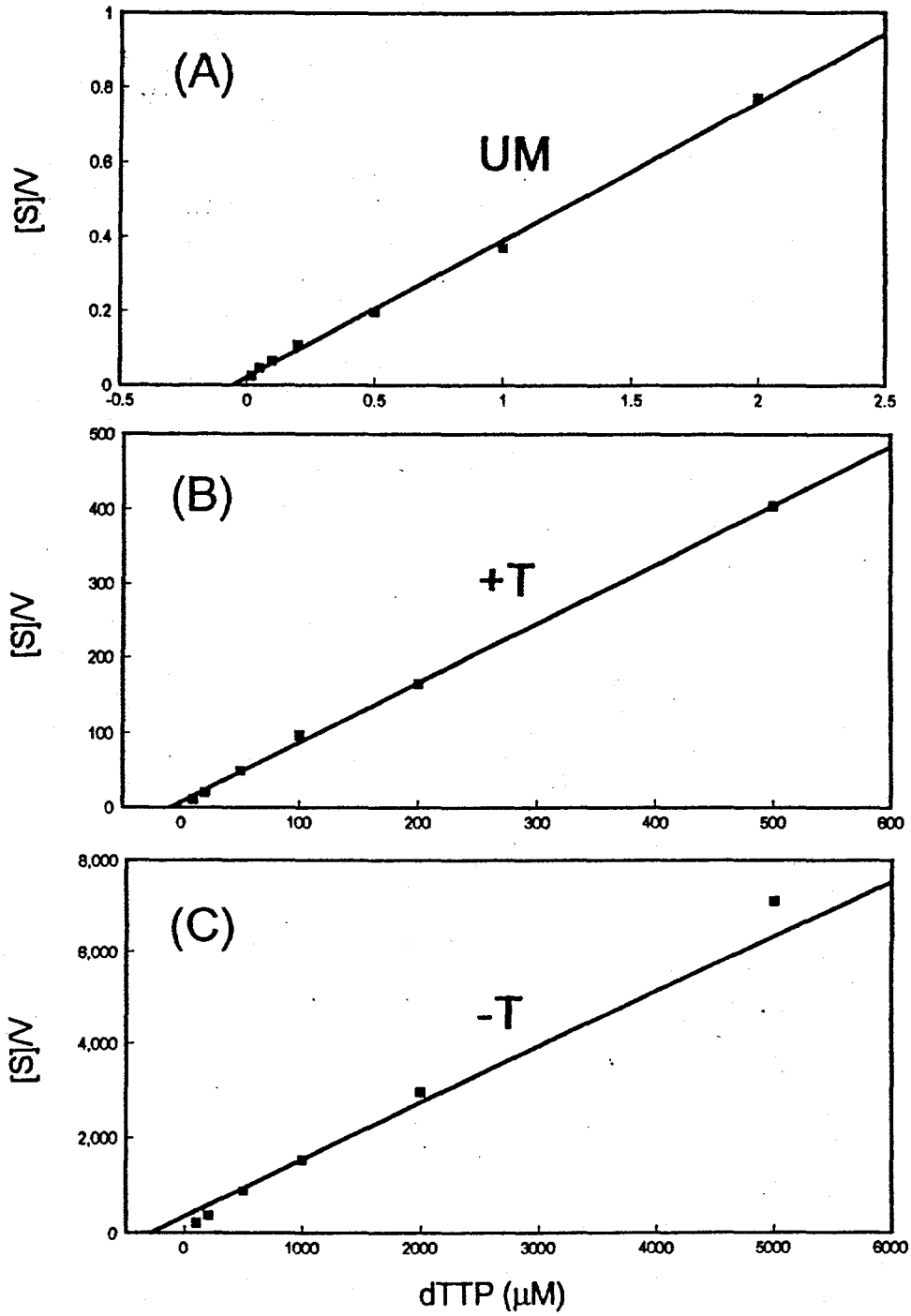

Figure 11 Hanes-Woolf plots for determining K_m and V_{max} for insertion of dTTP opposite the lesion site

(A) unmodified oligonucleotide template

(B) (+)-trans-B[c]PhDE adducted template

(C) (-)-trans-B[c]PhDE adducted template

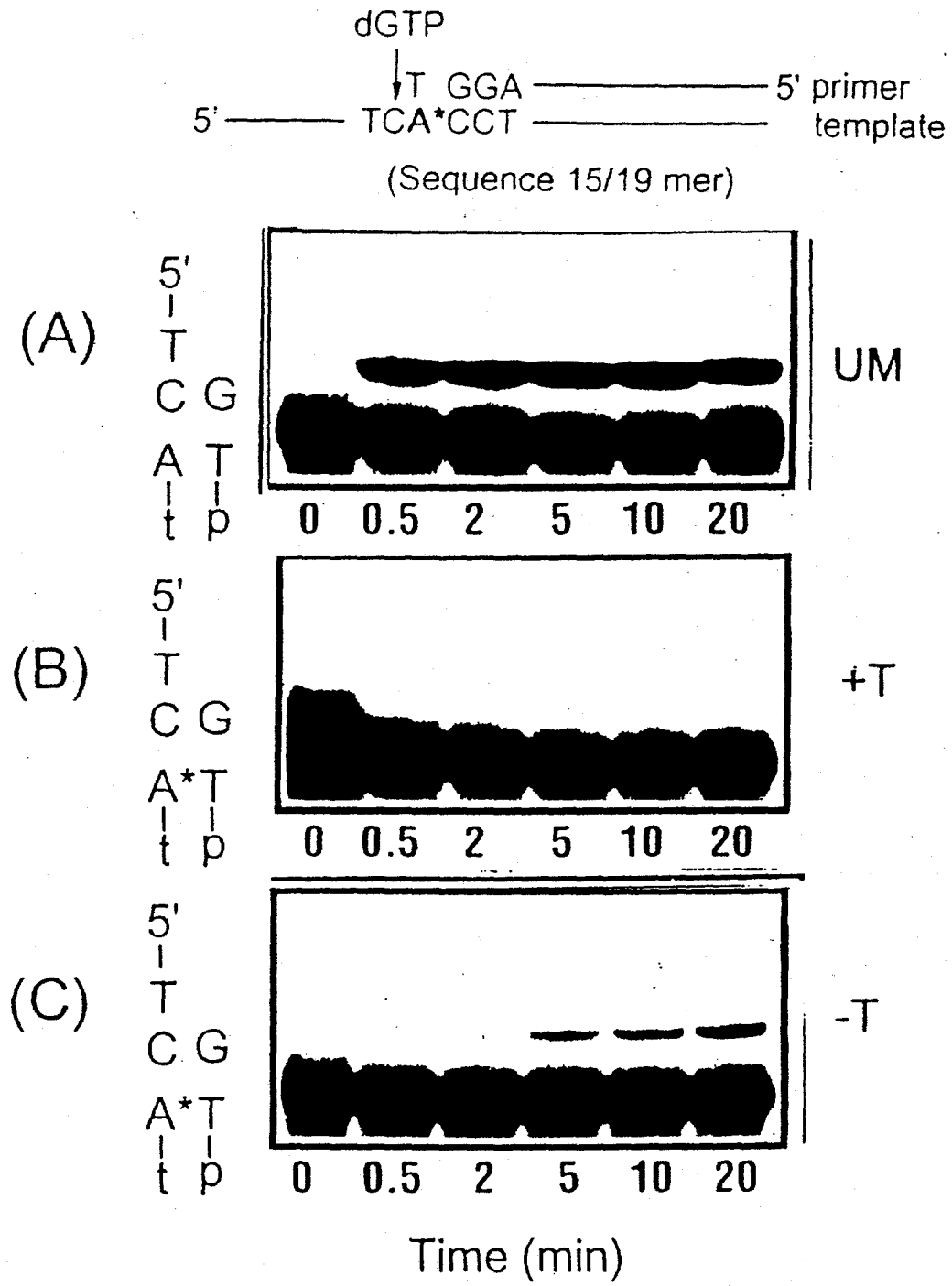

Figure 12 Gel autoradiogram showing the insertion of dGTP after the lesion site as a function of reaction time. Only dGTP is present as substrate in the reaction mix, [template/primer] = 100 nM, [enzyme] = 5.2 nM.

(A) unmodified oligonucleotide template, [dGTP] = 0.5 μM.

(B) (+)-trans-B[c]PhDE-dA modified oligonucleotide template, [dGTP] = 2 μM.

(C) (-)-trans-B[c]PhDE-dA modified oligonucleotide template, [dGTP] = 2 μM.

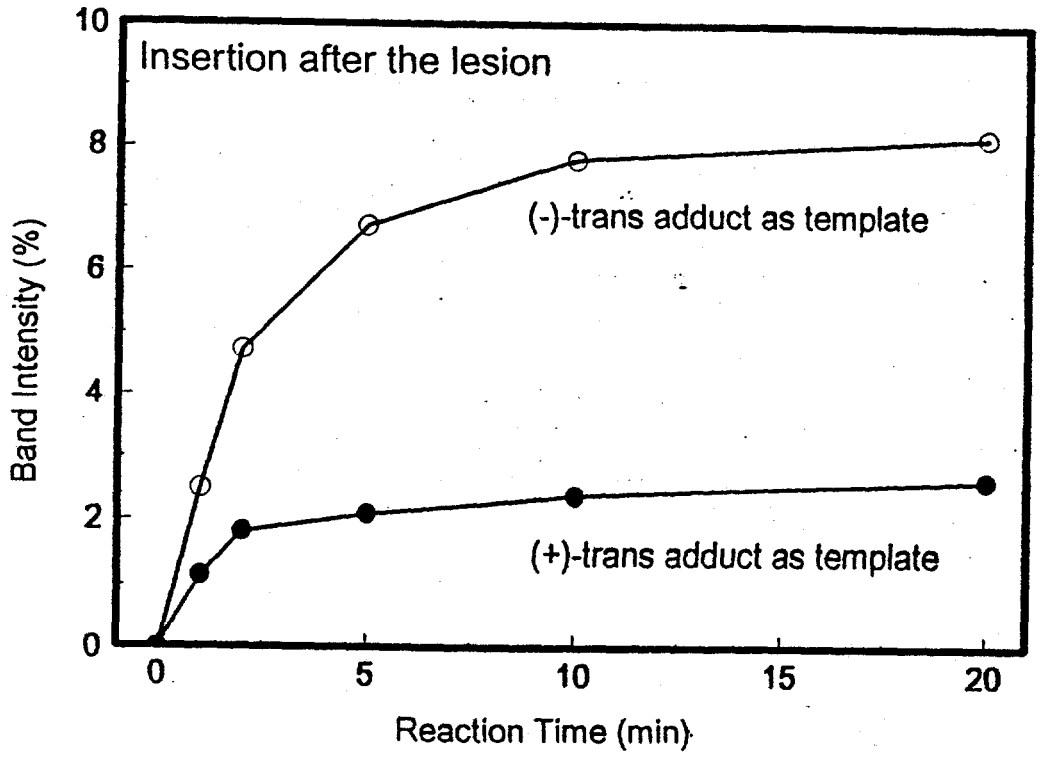

Figure 13 Relative band intensities of extended primer as a function of reaction time for the dGTP insertion after the lesion site (data taken from the gels depicted in Figure 12. The intensity values for each band are expressed as a percentage of the overall band intensities as defined in the legend to Figure 7.

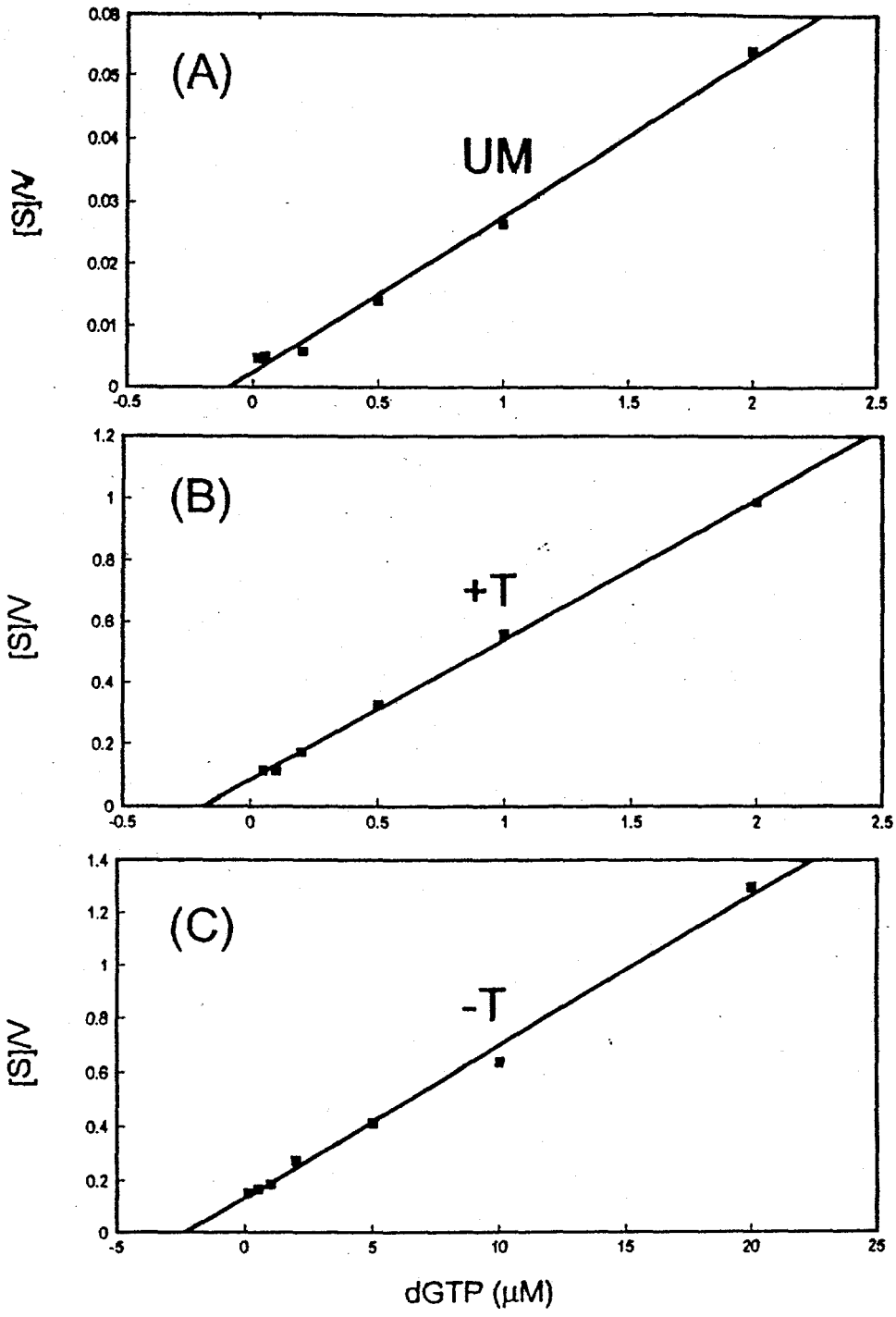

Figure 14 Hanes-Woolf plots for determining K_m and V_{max} for the insertion of dGTP after the lesion site

(A) unmodified oligonucleotide template

(B) (+)-trans-B[c]PhDE adducted template

(C) (-)-trans-B[c]PhDE adducted template

(+)-*trans*-adduct (f = 12) than for the (-)-*trans*-adducted template (f = 6.1) mainly because of the higher apparent dGTP binding affinity for the (+)-*trans*- (K_m = 0.20) than for the (-)-*trans*-adduct case (K_m = 3.3).

The difference in the apparent site-specific rate of DNA synthesis measured opposite the base flanking the modified dA residue on the 5'-side is consistent with the assumed orientation of the bulky B[c]PhDE residue on the 5'-side of the lesion in the (+)-trans-, and on the 3'-side in the case of the (-)-*trans-anti*-B[c]PhDE-N^6-dA lesion.

5. Discussion

5.1 Effects of B[c]PhDE-dA adduct stereochemistry

The effects of B[c]PhDE-N^6-dA adduct stereochemistry on the polymerase-catalyzed DNA synthesis rates can be discussed in terms of the three parameters, V_{max}, K_m , and f (V_m/K_m). We first consider the parameter V_{max}, the velocity of the DNA polymerase reaction when the substrate S is present in excess (reaction rate not limited by the binding and dissociation of dNTP from the enzyme-primer-template complex). If it is assumed that the adduct conformation, in particular the orientations of the B[c]PhDE residues relative to the adenosine residues to which they are bound, are similar in duplex DNA (Fig. 2) and at replicative primer/template junctions in polymerase complexes, then a correlation can be made between adduct conformation and V_{max}. Insertion of dGTP on the 3'-side of the modified guanine (insertion before the lesion, sequence 13/19mer) is more hindered in the case of the (-)-*trans* adduct than in the case of the (+)-*trans* adduct. The 3-fold lower of V_{max} for the (-)-*trans* adduct can be attributed to the pyrenyl residue pointing toward the 3'-direction of the template strand, thus sterically hindering the formation of the phosphodiester bond. However, in the case of the (+)-*trans* adduct, the pyrenyl residue points toward the 5'-direction of the template strand; thus, insertion of a dNTP *before* the lesion is expected to be less hindered than in the (-)-*trans*-adducted template, as observed.

In the case of incorporation of dGTP on the 5'-side of the modified guanine (extension after the lesion), V_{max} of the (-)-*trans* adduct is 8-fold higher than that of the (+)-*trans* adduct. This effect is opposite to the one observed in the case of the insertion of dGTP just before the lesion, and can also be explained by the opposite orientations of the B[c]PhDE residues with respect to the modified dA residue.

The values of K_m denote the ratio of (k_{-1} + k_{cat}) / k_1 of the dNTP-enzyme-DNA complex in the Michaelis-Menten equation. K_m is very close to the dissociation equilibrium constant because k_{-1} is likely to be greater than k_{cat}. The greater the K_m value, the less probable the binding of the dNTP to the enzyme-DNA complex. In all experiments, the K_m values of (+)-*trans* and (-)-*trans* adducts are greater than those of the unmodified templates, particularly in the case of insertion of dTTP opposite to the lesion; in that case, the K_m value for the unmodified template is at least 200-fold smaller than the K_m values for the B[c]PhDE-modified templates. This suggests that the binding of dNTP to the enzyme-DNA complex is severely disrupted by the presence of the bulky B[c]PhDE residue on the template strand.

It is known that the binding site for dNTP is located in the polymerase active site

(Kornberg and Baker, 1991; Beese et al., 1993). If the polymerase reaction occurs in the vicinity of the bulky B[c]PhDE residue (insertion before the lesion and extension after the lesion for sequences 13/19mer and 15/19mer), the binding of dNTP decreases to a lesser extent (2-10 fold increase in K_m). Since the bulky B[c]PhDE residue is closer to the dNTP binding site at the polymerase active site (insertion opposite the lesion for the 14/19mer sequence), it severely disrupts the binding of dNTP to the enzyme-DNA complex (200 fold increase in K_m). The K_m values for the (-)-B[c]PhDE-modified template is greater than for the (+)-*trans*-modified template in all experiments, suggesting that the (-)-*trans* lesion disrupts the binding of dNTP to a greater extent than the (+)-*trans* lesion. One reason for this may be the orientation of the (-)-*trans*-B[c]PhDE residue towards the 3'-side, and towards the 5'-side relative to the modified dA residue in the (+)-*trans*-B[c]PhDE-modified template. We can therefore expect that the integrity of the double-stranded region in the vicinity of the modified dA residue will be more disturbed in the (-)-*trans*- than in the (+)-*trans*-adduct case, thus accounting for the overall lower efficiency of DNA synthesis in the case of the (-)-B[c]PhDE-modified template.

The ratio of V_{max}/K_m (f) for the dNTP substrates indicates the efficiency with which each nucleotide base dNTP is inserted by the polymerase into the primer strand. When the polymerase reaction occurs near (before or after) the lesion site where the bulky residue is positioned, the nucleotide incorporation efficiency is reduced. For example, the efficiency of insertion before the lesion is reduced by 6-45 fold, and the efficiency of extension after the lesion is reduced by 30-60 fold. When the polymerase reaction occurs at the lesion site, the efficiency is reduced by 400-fold for the (+)-*trans* adduct, and by a factor of 10^4 in the case of the (-)-*trans* adduct. Thus, both lesions strongly inhibit DNA replication, and the inhibition by the (-)-*trans* lesion is 10 times greater than inhibition by the (+)-*trans* lesion.

5.2 Interpretation of Michaelis-Menten Parameters

A better understanding of the steady-state parameters K_m, V_{max} and V_m/K_m , and their relationships to the conformations of the B[c]PhDE lesions, can be obtained by analyzing the classical Michaelis-Menton kinetics on a more detailed level. From a series of pre-steady-state kinetic studies (Kuchta et al., 1987; 1988; Mizrahi et al., 1985; Dahlberg and Benkovic, 1991), Benkovic and coworkers have outlined a detailed kinetic pathway of DNA replication by the *E.coli* Pol I Klenow fragment:

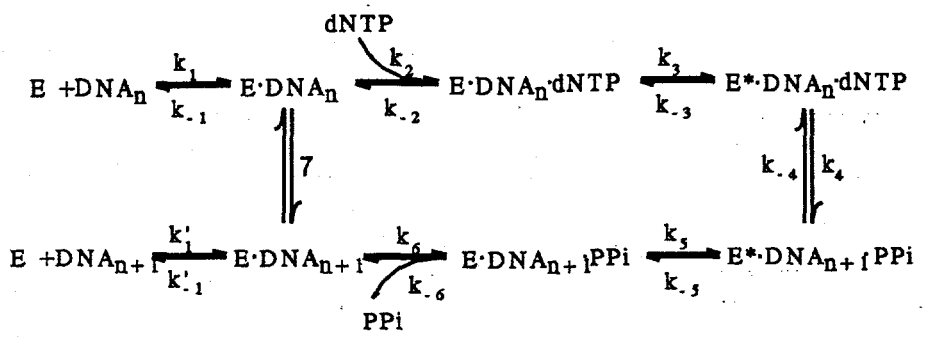

Figure 15. Kinetic Scheme of Klenow Mechanism

DNAn = template-primer, DNA n+1= template-primer extended by one nucleotide, E= Klenow fragment of *E.coli* DNA Pol I, E* = conformational change in enzyme

As illustrated in Fig. 15, in the forward direction for the proposed reaction pathway, DNA binding (k_1) precedes productive binding of dNTP to the enzyme (k_2). The polymerase then undergoes a conformational change (k_3) to a form E* which is poised for the catalysis of phosphodiester bond formation (k_4). Following dNTP addition, the enzyme undergoes a second conformational change (k_5) before pyrophosphate release (k_6) . At this point in the reaction, DNA can either dissociate from the polymerase (k'_{-1}) for a single nucleotide incorporation event, or remain bound for another cycle of dNTP addition (7) for processive synthesis. Comparing this kinetics pathway with classical Michaelis-Menten kinetics, the steady-state parameter K_m should be a good measure of K_D (k_2/k_{-2}), the dissociation constant of the enzyme-DNA-dNTP complex, and k_{cat} is a function of a series of microstep rate constants, k_3, k_4, k_5, k_6, $k_{-1'}$. k_{cat} can be calculated as $k_{cat} = V_{max}/[E]_0$, where $[E]_0$ is the total concentration of enzyme in the steady-state experiment. Thus, V_{max} can be influenced by a number of rates in this kinetics scheme, e.g., the rate of conformational change of enzyme (k_3), the rate of the chemical step (k_4), and the rate of dissociation of the enzyme from the product ($k_{-1'}$).

There are several possible control points in the nucleotide insertion pathway that are likely to be important in determining the dNTP insertion efficiency. These factors include the length of time that a dNTP remains bound to an enzyme-DNA complex (k_2 and k_{-2}), the enzyme conformational change (k_3), and the rate of phosphodiester bond formation (k_4). In the first stage of the reaction, the dNTP substrate-binding stage, the length of time that the substrate-enzyme-DNA complex remains stable may be determined by nonspecific nucleotide binding at the polymerase dNTP binding site, hydrogen bonding between the incoming dNTP and the template bases, and nearest neighbor base-stacking interactions (Echols and Goodman 1991). It is likely that the bulky B[c]PhDE residue adversely affects these three factors, and thus decreases the stability of the substrate-enzyme-DNA complex. When the bulky B[c]PhDE residue is near the polymerization site, K_m increases by 2-30 fold (The 13/19mer and the 15/19mer sequences). When the B[c]PhDE residue is at the polymerization site (the 14/19mer sequence), K_m increases by a much greater factor (500 to 10000-fold, Table 1). This suggests

that when the bulky B[c]PhDE residue is closer to the polymerase site as in the case of sequence 14/19mer, the stability of substrate-enzyme-DNA complex is more likely to be disturbed. In the 14/19mer sequence, the presence of the bulky B[c]PhDE residue in the substrate-enzyme-DNA complex substantially weakens nucleotide binding at the polymerase dNTP binding site, probably by weakening dNTP-template hydrogen bonding and base stacking interactions.

The maximum rate of nucleotide incorporation, k_{cat}, is limited by any of the elementary steps that follow dNTP binding (Figure 15), e.g. the conformational change (k_3), formation of the phosphodiester bond (k_4), or dissociation of the E-DNA_{n+1} (k_{-1}') complex. If the steady-state kinetics are measured properly during processive synthesis under conditions such that the DNA dissociation rate (k_{-1}') does not limit the net rate, then the maximum rate, k_{cat}, should be equal to k_3, the rate of the conformational change (Johnson, 1993; Dahlberg and Benkovic 1991). However, when a single correct nucleotide is incorporated, the rate-limiting step is the dissociation of the DNA_{n+1} product from the enzyme-DNA_{n+1} complex (Kuchta et. al., 1987). The k_{cat} value and k_{-1}' values were determined to be the same ($k_{cat} = k_{-1}'$), and range from 0.06 s^{-1} to 0.2 s^{-1} , depending on the DNA sequence in steady-state and pre-steady-state experiments (Kuchta et. al. 1987). Our k_{cat} data obtained from single nucleotide incorporation experiments on unmodified templates are 0.16 s^{-1}, 0.0054 s^{-1}, and 0.11 s^{-1} for the 13/19mer, 14/19mer, and 15/19mer sequences, respectively, in good agreement with those reported by Kuchta and co-workers (see Table 2 for the calculations of k_{cat}).

The rate of dissociation of the product from the enzyme-DNA complex (k_{-1}') for B[c]PhDE-modified templates should be faster or at least not slower than for the unmodified DNA since the enzyme-B[c]PhDE-modified template/primer complex is likely to be less stable than the enzyme-unmodified template/primer complex. If the rate-limiting step is the enzyme-DNA dissociation in the case of the B[c]PhDE-modified template/primer adducts ($k_{cat} = k_{-1}'$), one might expect the k_{cat} values for the modified DNA to be greater than for the unmodified template in steady-state experiments. In contrast, our data show that the k_{cat} values for adducts in all three sequences are lower than for the corresponding unmodified templates (Table 2). The lower k_{cat} values ($k_{cat} < k_{-1}'$) of nucleotide incorporation for B[c]PhDE-modified DNA templates suggest that the maximum rate of the polymerase reaction, k_{cat}, is not limited by the rate of enzyme-DNA dissociation, k_{-1}', but rather depends on the rate of the conformational change (k_3), at least in part. Direct proof that the enzyme-DNA dissociation is not rate-limiting in the case of the B[c]PhDE-modified DNA can be obtained by pre-steady-state experiments which was beyond the scope of this work. It is interesting to note that in the DNA replication study on AF and AAF adducts, the evidence from both steady-state and pre-steady-state experiments indicate that the rate of dNTP (k_{cat}) incorporation opposite or just after the adduct is of the same order as, or is significantly slower, than the enzyme-DNA dissociation rate constant, k_{-1}' (Lindsley and Fuchs, 1994).

The rate constant for the conformational change of the enzyme (k_3) which occurs after the initial binding of dNTP, but precedes the chemical step, is thought to be critical for the fidelity of DNA replication. It might involve postbinding selection for the correct geometry by an induced-fit mechanism. The enzyme is able to reach the catalytic configuration only if the newly formed base pair can adopt the Watson-Crick geometry, and if the chemical step

proceeds very rapidly. If these very rigid geometrical constraints cannot be attained, e.g., the bound dNTP and the template are not Watson-Crick paired, then the chemical reaction (k_4) proceeds very slowly and becomes the dominant rate-limiting step.

The B[c]PhDE residue on the template strand clearly distorts the preferred geometrical alignment in the enzyme complex. This adversely affects the enzyme conformational change, as well as the succeeding chemical step of phosphodiester bond formation, thereby altering the rate constant k_{cat}. These considerations may account for the observed correlations of the k_{cat} values obtained from the steady-state experiment with the orientations of the B[c]PhDE residues relative to the modified deoxyadenosine residues. This correlation can be explained as follows: whenever the B[c]PhDE residue is positioned in the vicinity of the polymerization site, it decreases the k_{cat} value; for example, when nucleotide incorporation occurs at the 3'-side of the modified dA (the 13/19mer sequence), the k_{cat} value is 3-fold smaller in the case of the (-)-*trans* adduct than in the case of the (+)-*trans*-adduct because the (-)-*trans*-B[c]PhDE residue points toward the 3'-side of the lesion, closer to the polymerization site. In the case of the (+)-*trans*-B[c]PhDE-modified template on the other hand, the B[c]PhDE residue points towards the 5'-side, away from the polymerization site. The opposite correlation between k_{cat} and the orientation of the B[c]PhDE can also be rationalized for extension of the primer strand by dNTP insertion just after the lesion, on the 5'-side of the modified dA residue (The 15/19mer sequence).

6. Conclusions

From the above, it is evident that the stereochemistry-dependent conformations of the B[c]PhDE-DNA lesions exhibit a remarkable influence on the activities of a typical prokaryotic DNA polymerase. These effects can be, in part, dissected by steady-state Michaelis-Menten kinetics. The general decrease in the base insertion efficiency (f) for B[c]PhDE adducts can be attributed to higher K_m and lower V_{max} values. In the detailed kinetic scheme, the B[c]PhDE lesion may disrupt the initial binding of dNTP to the active site of the polymerase causing higher K_m values , thus inhibiting the conformational changes of the enzyme that are so critical to its normal function, thus inhibiting the rate of phosphodiester bond formation.

The orientations of the covalently bound B[c]PhDE residues in the 1*R* (+)- and 1*S* (-)-*trans-anti*-B[c]PhDE-N^6-dA lesions on the template strand, diminish the values of V_{max} in a site-specific manner that is consistent with simple steric hindrance effects associated with the bulky B[c]PhDE residues. These effects are summarized in Fig. 16. In the 1*S* adduct, the B[c]PhDE residue points toward the 3'-end of the template strand and thus diminishes the reaction velocity V_{max} just before the lesion to a greater extent than the 1*R* adduct in which the B[c]PhDE residue points towards the opposite, 5'-direction. Consistent with this steric hindrance model, for extension of the primer strand just after the lesion site, V_{max} is lower for the 1*R* adduct than for the 1*S* adduct (Fig. 16).

The next step will be to investigate DNA polymerase kinetic parameters for the incorporation of the incorrect bases opposite to the lesion, and on either side of the modified base on the template strand. These studies, when correlated with ongoing conformational

studies of carcinogen-modified DNA template/primer complexes, would provide critical new mechanistic insights into the mechanisms by which these genotoxic chemicals cause mutations.

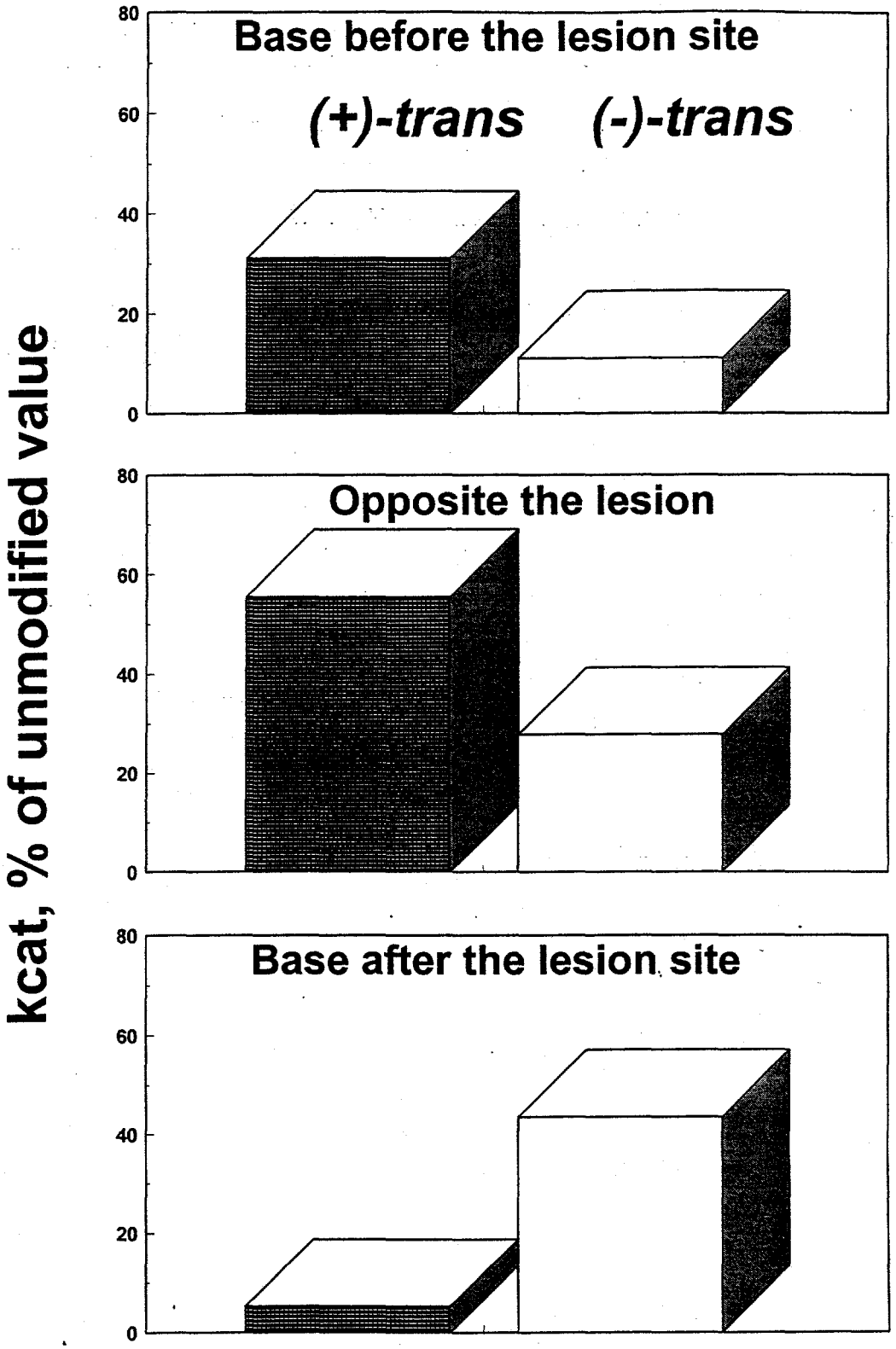

Figure 16 Summary of catalytic rate constants, kcat, for the addition of single dNTP's to a primer strand, catalyzed by E. coli POl I (Klenow fragment). The normal bases were added to the primer using the bases before, opposite, and after the lesion as templates.

Table 1. Kinetic Parameters for Single Nucleotide Incorporation Catalyzed by the Exonuclease-free Klenow fragment

Template	V_{max} (%/min)	K_m (μM)	f (V_{max}/K_m)
Incorporation of dGTP before the lesion site (Sequence 13/19 mer)			
unmodified oligomer	34 ± 1	0.12 ± 0.02	280 ± 56
(+)-*trans*-B[c]PhDE adduct	11 ± 1	0.24 ± 0.05	46 ± 14
(-)-*trans*-B[c]PhDE adduct	3.9 ± 0.1	0.64 ± 0.05	6.1 ± 0.6
Incorporation of dTTP opposite the lesion site (Sequence 14/19 mer)			
unmodified oligomer	2.5 ± 0.3	0.07 ± 0.02	36 ± 14
(+)-*trans*-B[c]PhDE adduct	1.3 ± 0.1	15 ± 2	0.087 ± 0.018
(-)-*trans*-B[c]PhDE adduct	0.72 ± 0.16	220 ± 40	0.0033 ± 0.0013
Incorporation of dGTP after the lesion site (Sequence 15/19 mer)			
unmodified oligomer	44 ± 6	0.12 ± 0.03	370 ± 140
(+)-*trans*-B[c]PhDE adduct	2.4 ± 0.2	0.20 ± 0.01	12 ± 2
(-)-*trans*-B[c]PhDE adduct	20 ± 1	3.3 ± 0.4	6.1 ± 1.0

The kinetic parameters were determined from at least two independent experiments.

Table 2. Calculation of Steady-state Catalytic Constant k_{cat}

Template	V_{max} (%/min) [a]	V_{max} (nM/s) [b]	E_0 (nM)[c]	k_{cat} (s^{-1}) [d]
Incorporation of dGTP before the lesion site (Sequence 13/19 mer)				
unmodified oligomer	34	0.57	3.4	0.17
(+)-*trans*-B[c]PhDE adduct	11	0.18	3.4	0.053
(-)-*trans*-B[c]PhDE adduct	3.9	0.065	3.4	0.019
Incorporation of dTTP opposite the lesion site (Sequence 14/19 mer)				
unmodified oligomer	2.5	0.042	7.8	0.0054
(+)-*trans*-B[c]PhDE adduct	1.3	0.022	7.8	0.003
(-)-*trans*-B[c]PhDE adduct	0.72	0.012	7.8	0.0015
Incorporation of dGTP after the lesion site (Sequence 15/19 mer)				
unmodified oligomer	44	0.73	52	0.11
(+)-*trans*-B[c]PhDE adduct	2.4	0.040	52	0.0058
(-)-*trans*-B[c]PhDE adduct	20	0.33	52	0.048

a. V_{max} (%/min) values are obtained from Table 1
b. V_{max} (%/min) values are converted to V_{max} (nM/s) using :
V_{max} (nM/s) = V_{max} (%/min) • 1/100 • 100nM • 1/60
where 100 nM is the primer concentration in all experiments
c. $[E]_0$ is the initial concentration of exo⁻ Klenow fragment in the reaction mixture
d. k_{cat} values are calculated using: $k_{cat} = V_{max} / [E]_0$

REFERENCES

Agarwal, S. K., Sayer, J. M., Yeh, H. J. C., Pannell, L. K., Hilton, B. D., Pigott, M. A., Dipple, A., Yagi, H. and Jerina, D. M. (1987) *J. Am. Chem. Soc.* 109, 2497-2504.

Agarwal, R., Canella, K.A., Yagi, H., Jerina, D.M., and Dipple, A. (1996) *Chem. Res. Toxicol. 9,* 586-592.

Beese, L. S., Friedman, J. M., and Steitz, T. A. (1993) *Biochemistry* 32, 14095-14101.

Bigger, C. A. H., Strandberg, J., Yagi, H., Jerina, D. M. and Dipple, A. (1989*) Proc. Natl. Acad. Sci. USA* 86, 2291-2295.

Bigger, C. A. H., John, J., Yagi, H., Jerina, D. M.and Dipple, A. (1992) *Proc. Natl. Acad. Sci. USA* 89, 368-372.

Boosalis, M.S., Petruska, J., and Goodman, M.F. (1987) *J. Biol. Chem.* 262, 14689-14696.

Carroll, S.S. and Benkovic, S. J. (1990) *Chem. Rev.* 90, 1291-1307.

Christner, D. F., Lakshman, M. K., Sayer, J. M., Jerina, D. M. and Dipple, A. (1994) *Biochemistry* 33, 14297-14305.

Conney, A. H. (1982) *Cancer Res.* 42, 4875-4917.

Cosman, M., de los Santos, C., Fiala, R., Hingerty, B. E., Ibanez, V., Margulis, L. A., Live, D., Geacintov, N. E., Broyde, S. and Putel, D. J. (1992) *Proc Natl. Acad. Sci USA*.89, 1914-1918.

Cosman, M., Fiala, R., Hingerty, B., Laryea, A., Lee, H., Harvey, R. G., Amins, S., Geacintov, N. E., Broyde, S. and Patel, D. J. (1993) *Biochemistry* 32, 12488-12497.

Cosman, M., Laryea, A., Fiala, R., Higerty, B. E., Amin, S., Geacintov, N. E., Broyde, S. and Patel, D. J. (1995a) *Biochemistry* **34**, 1295-1302.

Cosman, M., Hingerty, B., Geacintov, N.E., Broyde, S., and Patel, D.J. (1995b) *Biochemistry* **34**, 15334-15350.

de los Santos, C., Cosman, M., Hingerty, B. E., Ibanez, V., Margulis, L.A., Geacintov, N. E., Brodye, S. and Putel, D. J. (1992) *Biochemistry* 31, 524-532.

Dahlberg, M. E. and Benkovic, S. J. (1991) *Biochemistry* 30, 4835-4843 Dipple, A., Pigott, M. A., Agarwal, S. K., Yagi, H., Sayer, J. M., Jerina, D. M. (1987) *Nature* 327, 535-536.

Dosanjh, M. K., Galeros, G., Goodman, M. F. and Singer, B. (1991)*Biochemistry* **30**, 11595-

11599.

Echols, H. and Goodman, M. F. (1991) *Annu. Rev. Biochem.* 60, 477-451.

Eger, B. T., Kuchta, R. D., Carroll, S. S., Benkovic, P. A., Dahlberg, M. E., Joyce, C. M. and Benkovic, S. J. (1991) *Biochemistry* 30, 1441-1448.

Einolf, H.J., Amin, S., Yagi, H., Jerina, D.M., and Baird, W.M. (1996) *Carcinogenesis* 17, 2237-2244.

Feng, B., Hingerty, B.E., Geacintov, N.E., Broyde, S., and Patel, D.J. (1997) *Biochemistry,* in press.

Fersht, A. (1985) *Enzyme structure and mechanism p98-p118.* Freeman Publications, San Francisco.

Ittah, Y., Thakker, D.R., Levin, W., Croisy-Delcey, M., Ryan, D. E., Thomas, P. E., Conney, A.H. and Jerina, D. M. (1983) *Chem.-Biol. Interactions* 45, 15-28.

Johnson, K. A. (1993) *Annu. Rev. Biochem.* 62, 685-713.

Kornberg, A., Lehman, I. R., Bessman, M. J. and Simms, E. S. (1956) *Biochem. Biophys. Acta* 21, 197.

Kuchta, R. D., Mizrahi, V., Benkovic, P. A., Johnson, K. A. and Benkovic, S. J. (1987) *Biochemistry* 26, 8410-8417.

Kuchta, R. D., Benkovic, P. and Benkovic, S. J. (1988) *Biochemistry* 27, 6716-6725.

Laryea, A., Cosman, M., Lin, J-M., Liu, T. M., Agarwal, r., Smirnov, S., Amin, S., Harvey, R. G., Dipple, A. and Geacintov, N. E. (1995) *Chem. Res. Toxi.* **8**, 444-454.

Levin, W., Chang, R. L., Wood, A. W., Thakker, D. R., Yagi, H., Jerina, D. M. and Conney, A. H. (1986) *Cancer Res.* 46, 2257-2261.

Lindsley, J. E. and Fuchs, R. P. P. (1994) *Biochemistry* 33, 764-772.

Mao, B., Li, B., Amin, S., Cosman, M. and Geacintoc, N.E. (1993) *Biochemistry* 32, 11785-11793.

Mendelman, L. V., Boosalis, M. S., Petruska J. and Goodman, M. F. (1989) *J. Biol. Chem.* 264, 14415-14423.

Mendelman, L. V., Petruska, J. and Goodman, M. F. (1990) *J. Biol. Chem.* 265, 2338-2346.

Misra, B. and Amin, S. (1990) *J. Org. Chem.* 10, 1971-1974.
Ollis, D.L., Brick, P., Hamlin, R., Xuong, N.G. and Steitz, T.A. (1985) *Nature* 313, 762-766.

Mizrahi, V., Henrie, R. N., Marlier, J. F., Johnson, K. A., Benkovic, S. J.(1985) *Biochemistry* 24, 4010-4018.

Pruess-Schwartz, F., Baird, W.M., Yagi, H., Jerina, D. M., Pigott, M. A., Dipple, A. (1987) *Cancer Res.* 47, 4023-4037.

Randall, S.K., Eritja, R., Kaplan, B.E., Petruska, J., and Goodman, M.F. (1987) *J. Biol. Chem.* 262, 6864-6870.

Ross, H., Bigger, C.A. H., Yagi, H., Jerina, D.M.and Dipple, A. (1993) *Cancer Res.* 53, 1273-1277.

Shibutani, S., Margulis, L. A., Geacintov, N. E. and Grollman, A. P. (1993) *Biochemistry* 32, 7531-7541.

Singer, B., Chavez, F., Goodman, M. F., Essigmann, J. M. and Dosanjh, M. K. (1989) *Proc. Natl. Acad. Sci. USA* 86, 8271-8274.

Singer, B. and Dosanjh, M. K. (1990) *Mutation Research* 233, 45-51.

Thakker, D. R., Levin, W., Yagi, H., Yeh, H. J. C., Ryan, D. E., Thomas, P. E., Conney, A. H. and Jerina, D. M. (1986) *J. Biol. Chem.* 261, 5404-5413.

Wood, A. W., Chang, R. L., Levin, W., Yagi, H., Thakker, D. R., Sayer, J. M., Jerina, D. M. and Conney, A. H. (1984) *Ca37ncer Res.* 44, 2320-2324.

DISCLAIMER